

NASA
Technical
Paper
3363

August 1993

Nonperturbative Methods in HZE Ion Transport

John W. Wilson,
Francis F. Badayi,
Robert C. Costen,
and Judy L. Shinn

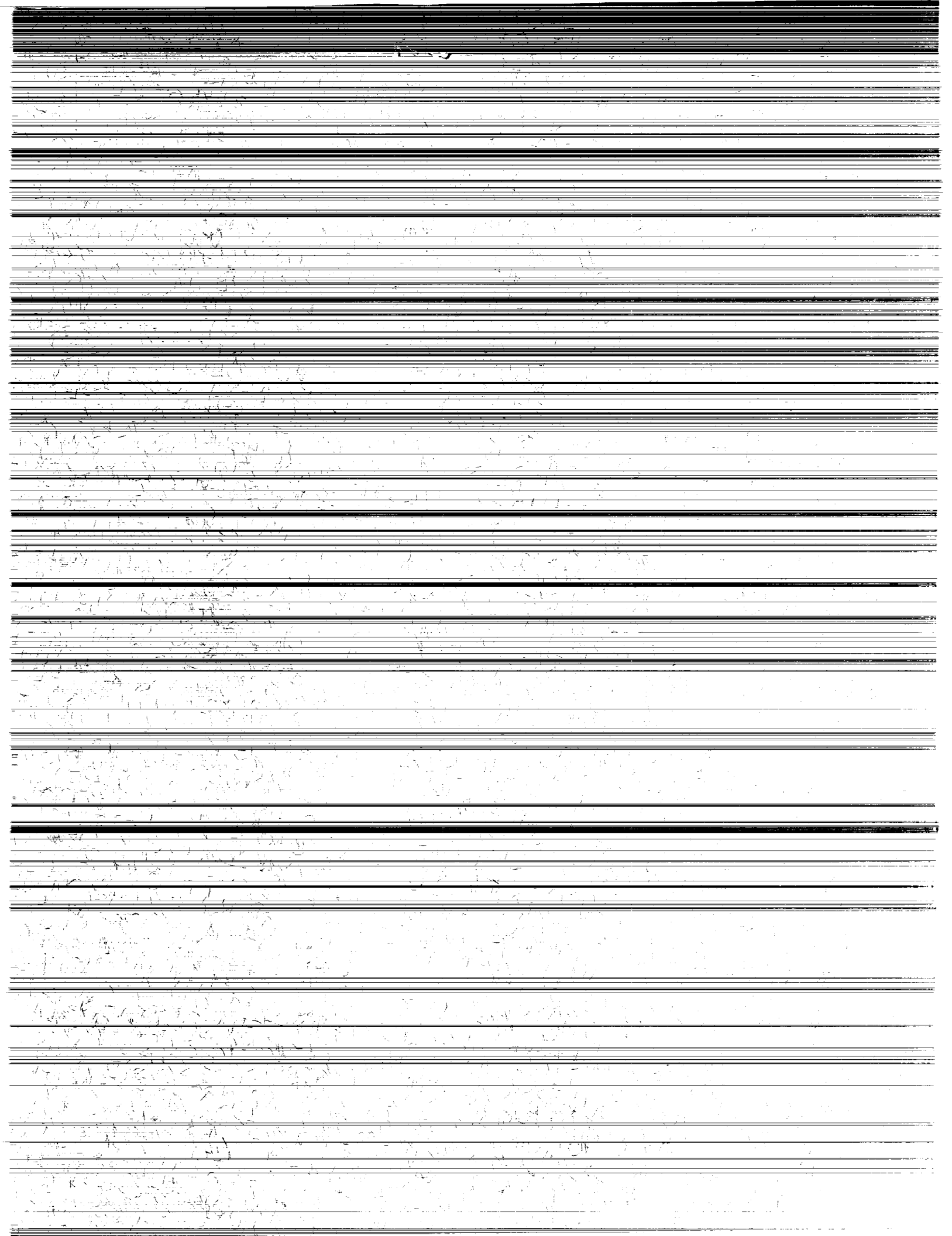
(NASA-TP-3363) NONPERTURBATIVE
METHODS IN HZE ION TRANSPORT
(NASA) 27 p

N94-10759

Unclas

H1/93 0185021

The NASA logo, consisting of the word "NASA" in a bold, sans-serif font, with a stylized "meatball" symbol above the letter "A".



**NASA
Technical
Paper
3363**

1993

Nonperturbative Methods in HZE Ion Transport

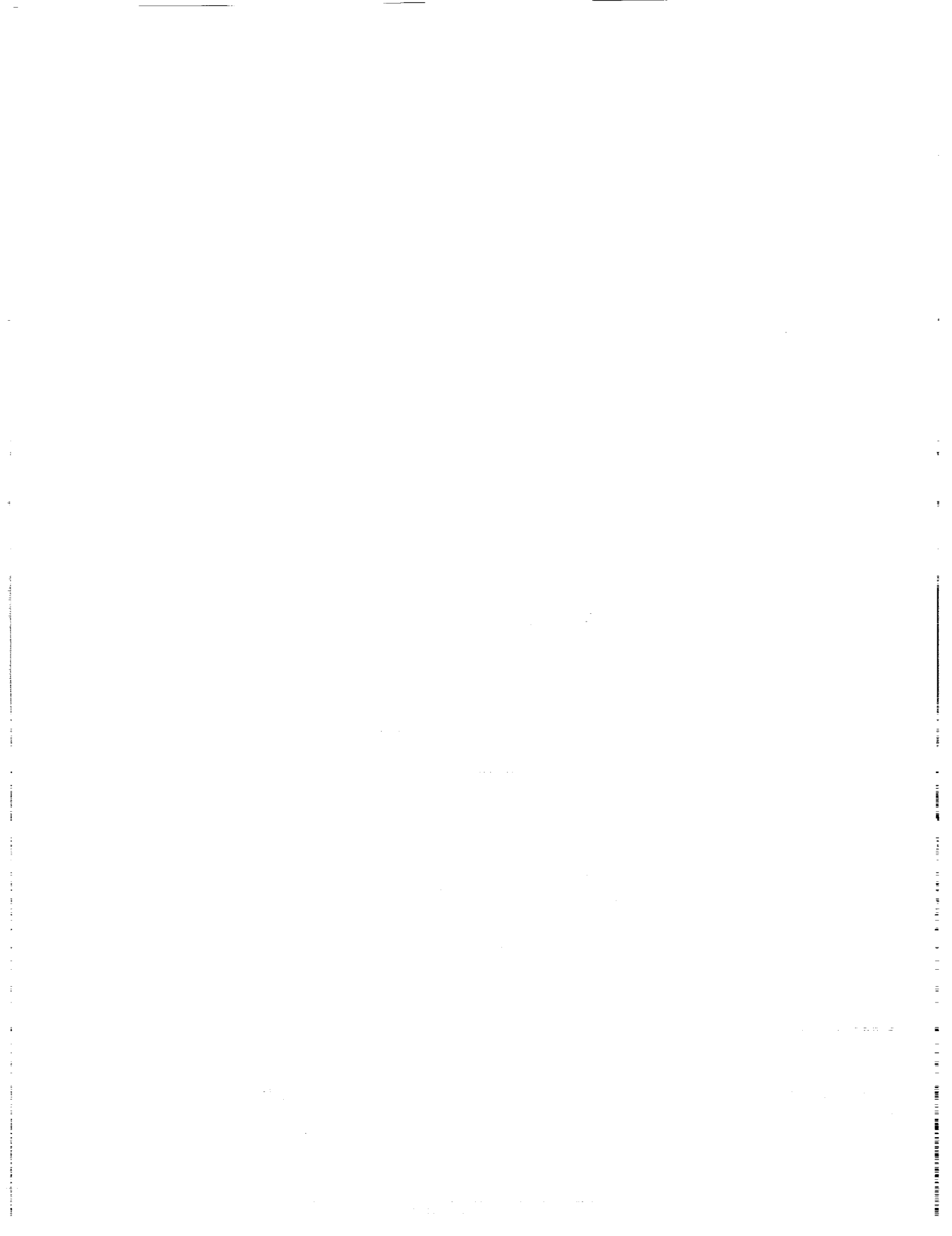
John W. Wilson
*Langley Research Center
Hampton, Virginia*

Francis F. Badavi
*Christopher Newport University
Newport News, Virginia*

Robert C. Costen
and Judy L. Shinn
*Langley Research Center
Hampton, Virginia*



National Aeronautics and
Space Administration
Office of Management
Scientific and Technical
Information Program



Abstract

A nonperturbative analytic solution of the high charge and energy (HZE) Green's function is used to implement a computer code for laboratory ion beam transport. The code is established to operate on the Langley Research Center nuclear fragmentation model used in engineering applications. Computational procedures are established to generate linear energy transfer (LET) distributions for a specified ion beam and target for comparison with experimental measurements. The code is highly efficient and compares well with the perturbation approximations.

Introduction

Green's function has been identified as the likely means of generating efficient high charge and energy (HZE) shielding codes for space engineering which are capable of being validated in laboratory experiments (ref. 1). A derivation of Green's function as a perturbation series was promising for development of a laboratory-validated engineering code (ref. 2), but computational inefficiency provided a major obstacle to code development (ref. 3). More recently, non-perturbative approximations to the HZE Green's function have shown promise in providing an efficient validated engineering code (ref. 4). Described herein is a laboratory code that uses a nonperturbation Green's function to derive LET spectra for ion beams with an atomic number $Z \leq 28$. These ions correspond to the major components of the galactic cosmic ray spectrum.

Theory

We restrict our attention to the multiple charged ions for which the Boltzmann equation may be reduced to

$$\left[\frac{\partial}{\partial x} - \frac{\partial}{\partial E} \tilde{S}_j(E) + \sigma_j \right] \phi_j(x, E) = \sum_k \sigma_{jk} \phi_k(x, E) \quad (1)$$

where $\phi_j(x, E)$ is the flux of ion type j at x with energy E (in MeV/amu), $\tilde{S}_j(E)$ is the change in E per unit distance, σ_j is the total macroscopic reaction cross section, and σ_{jk} is the macroscopic cross section for collision of ion type k to produce an ion of type j . (See refs. 1 to 5.) The solution to equation (1) is found subject to the boundary condition

$$\phi_j(0, E) = f_j(E) \quad (2)$$

which for laboratory beams has only one value of j for which $f_j(E)$ is not zero, and $f_j(E)$ is described

by a mean energy E_0 and energy spread σ such that

$$f_j(E) = \frac{1}{\sqrt{2\pi}\sigma} \exp \left[-\frac{(E - E_0)^2}{2\sigma^2} \right] \quad (3)$$

The usual method of solution is to proceed in solving equation (1) as a perturbation series (refs. 1 and 5). In practice the computational requirements limit the usefulness of the technique for deep penetration (ref. 3).

The Green's function is introduced as a solution of

$$\begin{aligned} \left[\frac{\partial}{\partial x} - \frac{\partial}{\partial E} \tilde{S}_j(E) + \sigma_j \right] G_{jm}(x, E, E_0) \\ = \sum_k \sigma_{jk} G_{km}(x, E, E_0) \end{aligned} \quad (4)$$

subject to the boundary condition

$$G_{jm}(0, E, E_0) = \delta_{jm} \delta(E - E_0) \quad (5)$$

where δ_{jm} is Kronecker's delta and $\delta(E - E_0)$ is Dirac's delta. The solution to equation (1) is given by superposition as

$$\phi_j(x, E) = \sum_k \int G_{jk}(x, E, E') f_k(E') dE' \quad (6)$$

If $G_{jk}(x, E, E')$ is known as an algebraic quantity, then equation (6) may be evaluated by simple integration techniques and the associated errors in numerically solving equation (1) are avoided (ref. 6).

The above equations can be simplified by transforming the energy into the residual range as

$$r_j = \int_0^E \frac{dE'}{\tilde{S}_j(E')} \quad (7)$$

and defining new field functions as

$$\psi_j(x, r_j) = \tilde{S}_j(E)\phi_j(x, E) \quad (8)$$

$$\mathcal{G}_{jm}(x, r_j, r'_m) = \tilde{S}_j(E)G_{jm}(x, E, E') \quad (9)$$

$$\hat{f}_j(r_j) = \tilde{S}_j(E)f_j(E) \quad (10)$$

Equation (4) becomes

$$\begin{aligned} & \left(\frac{\partial}{\partial x} - \frac{\partial}{\partial r_j} + \sigma_j \right) \mathcal{G}_{jm}(x, r_j, r'_m) \\ &= \sum_k \frac{\nu_j}{\nu_k} \sigma_{jk} \mathcal{G}_{km}(x, r_k, r'_m) \end{aligned} \quad (11)$$

with the boundary condition

$$\mathcal{G}_{jm}(0, r_j, r'_m) = \delta_{jm} \delta(r_j - r'_m) \quad (12)$$

and with the solution to the ion fields given by

$$\psi_j(x, r_j) = \sum_m \int_0^\infty \mathcal{G}_{jm}(x, r_j, r'_m) \hat{f}_m(r'_m) dr'_m \quad (13)$$

Note that ν_j is the range scale factor such that $\nu_j r_j = \nu_m r_m$ and can be expressed as $\nu_j = Z_j^2/A_j$. The solution to equation (11) is written as a perturbation series:

$$\mathcal{G}_{jm}(x, r_j, r'_m) = \sum_i \mathcal{G}_{jm}^{(i)}(x, r_j, r'_m) \quad (14)$$

where

$$\mathcal{G}_{jm}^{(0)}(x, r_j, r'_m) = g(j) \delta_{jm} \delta(x + r_j - r'_m) \quad (15)$$

and

$$\mathcal{G}_{jm}^{(1)}(x, r_j, r'_m) \approx \frac{\nu_j \sigma_{jm} g(j, m)}{x(\nu_m - \nu_j)} \quad (16)$$

where $\mathcal{G}_{jm}^{(1)}(x, r_j, r'_m)$ is zero unless

$$\frac{\nu_j}{\nu_m} (r_j + x) \leq r'_m \leq \frac{\nu_j}{\nu_m} r_j + x \quad (17)$$

for $\nu_m > \nu_j$. If $\nu_j > \nu_m$, as can happen in neutron removal, the negative of equation (16) is used and the upper and lower limits of equation (17) are switched. The higher terms are approximated as

$$\begin{aligned} & \mathcal{G}_{jm}^{(i)}(x, r_j, r'_m) \\ & \approx \sum_{k_1, k_2, \dots, k_{i-1}} \frac{\nu_j \sigma_{jk_1} \sigma_{k_1 k_2} \dots \sigma_{k_{i-1} m} g(j, k_1, k_2, \dots, k_{i-1}, m)}{x(\nu_m - \nu_j)} \end{aligned} \quad (18)$$

In the above equation,

$$g(j) = \exp(-\sigma_j x) \quad (19)$$

and

$$\begin{aligned} & g(j_1, j_2, \dots, j_n, j_{n+1}) \\ &= \frac{g(j_1, j_2, \dots, j_{n-1}, j_n) - g(j_1, j_2, \dots, j_{n-1}, j_{n+1})}{\sigma_{j_{n+1}} - \sigma_{j_n}} \end{aligned} \quad (20)$$

Note that $\mathcal{G}_{jm}^{(i)}(x, r_j, r'_m)$ is purely dependent on x for $i > 0$, and we represent this expression as $\mathcal{G}_{jm}^{(i)}(x)$. (See ref. 3.) In terms of equations (14) to (20), the solution to equation (1) becomes (ref. 3)

$$\begin{aligned} \psi_j(x, r_j) &= \exp(-\sigma_j x) \hat{f}_j(r_j + x) \\ &+ \sum_{m,i} \mathcal{G}_{jm}^{(i)}(x) \left[\hat{F}_m(r'_{m,\ell}) - \hat{F}_m(r'_{m,u}) \right] \end{aligned} \quad (21)$$

In equation (21), $r'_{m,u}$ and $r'_{m,\ell}$ are given by the upper and lower limits of equation (17). The symbol $\hat{F}_m(r'_m)$ refers to the integral spectrum

$$\hat{F}_m(r'_m) = \int_{r'_m}^\infty \hat{f}_m(r) dr \quad (22)$$

We note that

$$\hat{F}_m(r'_m) \equiv F_m(E') \quad (23)$$

with

$$F_m(E') = \int_{E'}^\infty f_m(E) dE \quad (24)$$

and

$$r'_m = \int_0^{E'} \frac{dE}{\tilde{S}_m(E)} \quad (25)$$

We now introduce nonperturbation terms for the summation in equation (21). First, we recall that the g -function of n arguments is generated by the perturbation solution of the transport equation neglecting ionization energy loss (ref. 1) given by

$$\left(\frac{\partial}{\partial x} + \sigma_j \right) g_{jm}(x) = \sum_k \sigma_{jk} g_{km}(x) \quad (26)$$

subject to the boundary condition

$$g_{jm}(0) = \delta_{jm} \quad (27)$$

The solution is

$$g_{jm}(x) = \delta_{jm}g(m) + \sigma_{jm}g(j, m) + \sum_k \sigma_{jk}\sigma_{km}g(j, k, m) + \dots \quad (28)$$

It is also true that

$$g_{jm}(x) = \sum_k g_{jk}(x-y)g_{km}(y) \quad (29)$$

for any positive values of x and y . Equation (29) may be used to propagate the function $g_{jm}(x)$ over the solution space, after which

$$g_{jm}(x, r_j, r'_m) \approx \exp(-\sigma_j x) \delta_{jm} \delta(x + r_j - r'_m) + \frac{\nu_j [g_{jm}(x) - \exp(-\sigma_j x) \delta_{jm}]}{x(\nu_m - \nu_j)} \quad (30)$$

The approximate solution of equation (1) is then given by

$$\psi_j(x, r_j) = \exp(-\sigma_j x) \hat{f}(r_j + x) + \sum_m \frac{\nu_j [g_{jm}(x) - \exp(-\sigma_j x) \delta_{jm}]}{x(\nu_m - \nu_j)} + [\hat{F}_m(r'_{m,u}) - \hat{F}_m(r'_{m,\ell})] \quad (31)$$

which is a relatively simple quantity (ref. 4).

Comparison With Perturbation Theory

The first step in testing the new code is comparing its results with the perturbation theory results. The perturbation code has been previously compared with ^{20}Ne transport experiments at the Lawrence Berkeley Laboratory (LBL) BEVALAC accelerator (refs. 7 and 8). The comparison required the use of acceptance functions to obtain detector response, and results of those comparisons are shown in figure 1. The dynamic range of the detector system was inadequate for the Be and B ions - especially at the lower depths. The results are thought to be within 30 percent over the dynamic range of ions for which the detectors were designed (ref. 8). The primary errors in the computation are attributed to the nuclear cross sections and approximations used in applying the acceptance functions. A sample LET spectrum for the C ions is shown in figure 2, which indicates excellent agreement between theory and experiment. The spectrum for the Ne ions is shown in figure 3. The agreement is less favorable since Ne fragment

isotopes have not been evaluated in the computations. (See ref. 8 for Ne fragment isotope effects at 15 cm.) The main uncertainty is believed to be the fragmentation cross sections. The only complete sets of fragmentation cross sections measured are for ^{12}C and ^{16}O projectiles at both 1.05 GeV/amu and 2.1 GeV/amu, and ^{20}Ne cross sections are obtained (ref. 9) as an extrapolation. The Ne, F, and N cross sections scaled according to reference 9 are among the more reliable unmeasured cross sections.

We converted the perturbation code to use the NUCFRAG data base (refs. 10 and 11). Direct comparison of the perturbation code and the non-perturbation Green's function code is then possible. Figure 4 shows the first collision term from both theories for a 600 MeV/amu ^{56}Fe beam at three depths in water. The differences in spectral shape are due to simplification of the attenuation term in the non-perturbation theory (ref. 1). The total ion flux of each type is the same as we have shown elsewhere (refs. 1 and 6). The nonperturbation term represents the average spectrum, while perturbation theory retains the spectral shape. The second collision terms are shown in figure 5. There is better spectral detail maintained in the perturbation code than in the nonperturbation code, but the same total ion flux for each ion type is obtained for both. The (approximate) third collision term of the perturbation theory is shown with the remaining nonperturbation terms in figure 6. The total ion fluxes for the two theories are nearly equal for heavy fragments but differ substantially for lighter fragments. By comparing figures 4, 5, and 6 we see that the sequence of perturbation terms appears to be converging to a result similar to the nonperturbation result. Although perturbation theory converges rapidly for the heavier fragments, the light fragment production from higher order terms is important for this heavy ion beam and cannot be neglected. This deficiency in accounting for light fragments is not a great concern since these terms are efficiently evaluated by the present non-perturbative techniques. Results for the first three terms of perturbation theory are compared with results for all terms of the nonperturbation theory in figure 7. The nonconvergence of the light fragments in the first three perturbation terms is most apparent by comparing results for the third-order and higher nonperturbation terms (fig. 6(c)) with results for the third-order perturbation term (fig. 6(d)), for example. Aside from the convergence issue, the computation time required for the nonperturbation code is approximately 10 minutes on a VAX 4000/500 system, compared with 15 minutes for evaluation of the first collision term, 45 minutes for the second

collision term, and 90 minutes for the third collision term for the perturbation code. We felt that little would be gained by evaluating the fourth term, which would require more computer time than the first three terms combined. In addition to the ^{56}Fe ion beam results given in figures 4 to 7, the nonperturbative method generates the Green's function for any ion at $Z \leq 28$ for any arbitrary initial energy. Each additional ion or energy requires an additional 150 minutes to evaluate the first three collision terms using the perturbation-based code. This should amply demonstrate the power of the nonperturbative solutions.

A Practical Green's Function Code

Although the nonperturbation Green's function provides a rapid computational method, the spectral terms are replaced by averages over the spectral domains of higher order terms. These average spectra can be easily corrected with the spectral distributions using perturbation theory. The first collision Green's function is given (ref. 2) as

$$\mathcal{G}_{jm}^{(1)}(x, r_j, r'_m) = \frac{\nu_j \sigma_{jm}}{|\nu_m - \nu_j|} \exp(-\sigma_j x_j - \sigma_m x_m) \quad (32)$$

We rewrite $\mathcal{G}_{jm}^{(1)}$ in terms of its average value (given by eq. (16)) as

$$\mathcal{G}_{jm}^{(1)}(x, r_j, r'_m) = \frac{\nu_j \sigma_{jm}}{\nu_m - \nu_j} \frac{g_{jm}^{(1)}(x)}{x} + b_{jm}(x)(r'_m - \bar{r}'_m) \quad (33)$$

where

$$\bar{r}'_m = \frac{r'_{m,\ell} + r'_{m,u}}{2}$$

is the midpoint \bar{r}'_m between its limits given by equation (17). The b_{jm} term of equation (33) has the property that

$$\int_{r'_{m,\ell}}^{r'_{m,u}} b_{jm}(x)(r' - \bar{r}'_m) dr' = 0 \quad (34)$$

to ensure that the first term of equation (33) is indeed the average spectrum as required. The spectral slope parameter is

$$b_{jm}(x) = \frac{\nu_j \nu_m \sigma_{jm} [\exp(-\sigma_m x) - \exp(-\sigma_j x)]}{x(\nu_m - \nu_j)|\nu_m - \nu_j|} \quad (35)$$

Results for the nonperturbation Green's function with spectral corrections are shown in figure 8 and should be compared with the results in figure 7. A similarly simple spectral correction could be made to

the higher order terms. The spectral correction given in equation (33) is included in the present Green's function code.

LET Spectra for Laboratory Beams

We use the boundary condition appropriate for laboratory beams given by equation (3). The cumulative spectrum is given by

$$F_j(E) = \frac{1}{2} \left[1 - \operatorname{erf} \left(\frac{E - E_o}{\sqrt{2}\sigma} \right) \right] \quad (36)$$

The cumulative energy moment needed to evaluate the spectral correction is

$$\begin{aligned} \bar{E}_j(E) &= \frac{1}{2} E_o \left[1 - \operatorname{erf} \left(\frac{E - E_o}{\sqrt{2}\sigma} \right) \right] \\ &+ \frac{\sigma}{\sqrt{2\pi}} \exp \left[-\frac{(E - E_o)^2}{2\sigma^2} \right] \end{aligned} \quad (37)$$

The average energy on any subinterval (E_1, E_2) is then

$$\bar{E} = \frac{\bar{E}_j(E_1) - \bar{E}_j(E_2)}{F_j(E_1) - F_j(E_2)} \quad (38)$$

The beam-generated flux is

$$\begin{aligned} \psi_j(x, r_j) &= \exp(-\sigma_j x) \hat{f}_j(r_j + x) \\ &+ \sum_{m,i} \mathcal{G}_{jm}^{(i)}(x) [\hat{F}_m(r'_{m,u}) - \hat{F}_m(r'_{m,\ell})] \\ &+ \sum_m b_{jm}^{(1)}(x) [r'_m(\bar{E}) - \bar{r}'_m] [\hat{F}_m(r'_{m,u}) - \hat{F}_m(r'_{m,\ell})] \end{aligned} \quad (39)$$

where \bar{E} is evaluated using equation (38) with E_1 and E_2 as the lower and upper limits associated with $r'_{m,\ell}$ and $r'_{m,u}$.

The differential fluence spectra for a 600 MeV/amu ^{56}Fe beam with a 2.5 MeV/amu standard deviation are shown in figure 9. The results in figure 9 are similar to those shown in figure 8 except the ends of the spectra are rounded by the energy spread of the primary beam. The LET distribution is found using the methods of reference 12. The corresponding LET spectra are shown in figure 10. The highest LET peak is due to the primary beam and the iron fragments. The successive peaks below iron are due to lower atomic weight fragments.

Concluding Remarks

The present analysis has resulted in a new transport code for high charge and energy (HZE)

ions which is a highly efficient nonperturbative analytic solution. Indeed, the basic solution for every ion through ^{58}Ni is generated in minutes on a VAX 4000 series computer. The solutions compare favorably with the perturbation series solutions, which have been validated to some extent in laboratory experiments with ^{20}Ne beams. The code holds promise of an efficient space engineering code that can be tested in laboratory experiments.

NASA Langley Research Center
Hampton, VA 23681-0001
June 23, 1993

References

1. Wilson, John W.; Lamkin, Stanley L.; Farhat, Hamidullah; Ganapol, Barry D.; and Townsend, Lawrence W.: *A Hierarchy of Transport Approximations for High Energy Heavy (HZE) Ions*. NASA TM-4118, 1989.
2. Wilson, John W.; Townsend, L. W.; Lamkin, S. L.; and Ganapol, B. D.: A Closed-Form Solution to HZE Propagation. *Radiat. Res.*, vol. 122, 1990, pp. 223-228.
3. Wilson, J. W.; and Badavi, F. F.: New Directions in Heavy Ion Shielding. *Proceedings of the Topical Meeting on New Horizons in Radiation Protection and Shielding*, American Nuclear Soc., Inc., 1992, pp. 198-202.
4. Wilson, John W.; Costen, Robert C.; Shinn, Judy L.; and Badavi, Francis F.: *Green's Function Methods in Heavy Ion Shielding*. NASA TP-3311, 1993.
5. Wilson, John W.: *Analysis of the Theory of High-Energy Ion Transport*. NASA TN D-8381, 1977.
6. Wilson, John W.; Townsend, Lawrence W.; Schimmerling, Walter; Khandelwal, Govind S.; Khan, Ferdous; Nealy, John E.; Cucinotta, Francis A.; Simonsen, Lisa C.; Shinn, Judy L.; and Norbury, John W.: *Transport Methods and Interactions for Space Radiations*. NASA RP-1257, 1991.
7. Schimmerling, Walter; Miller, Jack; Wong, Mervyn; Rapkin, Marwin; Howard, Jerry; Spieler, Helmut G.; and Jarrett, Blair V.: The Fragmentation of 670A MeV Neon-20 as a Function of Depth in Water. *Radiat. Res.*, vol. 120, 1989, pp. 36-71.
8. Shavers, Mark R.; Curtis, Stanley B.; Miller, Jack; and Schimmerling, Walter: The Fragmentation of 670A MeV Neon-20 as a Function of Depth in Water. II. One-Generation Transport Theory. *Radiat. Res.*, vol. 124, 1990, pp. 117-130.
9. Silberberg, R.; Tsao, C. H.; and Shapiro, M. M.: Semiempirical Cross Sections, and Applications to Nuclear Interactions of Cosmic Rays. *Spallation Nuclear Reactions and Their Applications*, B. S. P. Shen and M. Merker, eds., D. Reidel Publ. Co., c.1976, pp. 49-81.
10. Wilson, John W.; Townsend, Lawrence W.; and Badavi, F. F.: A Semiempirical Nuclear Fragmentation Model. *Nucl. Instrum. & Methods Phys. Res.*, vol. B18, no. 3, Feb. 1987, pp. 225-231.
11. Shinn, Judy L.; John, Sarah; Tripathi, Ram K.; Wilson, John W.; Townsend, Lawrence W.; and Norbury, John W.: *Fully Energy-Dependent HZETRN (A Galactic Cosmic-Ray Transport Code)*. NASA TP-3243, 1992.
12. Wilson, John W.; and Badavi, Francis F.: *A Study of the Generation of Linear Energy Transfer Spectra for Space Radiations*. NASA TM-4410, 1992.

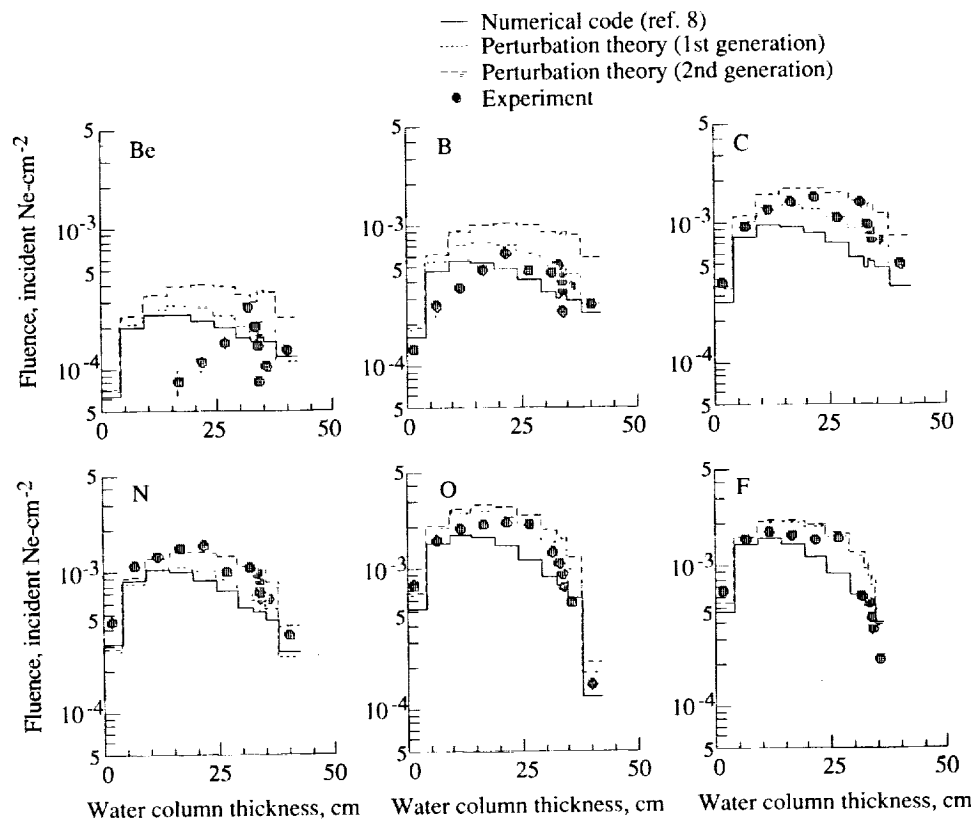


Figure 1. Integral fluence for all fragments produced by neon nuclei incident on various thicknesses of water as function of water column thickness. (From ref. 6.)

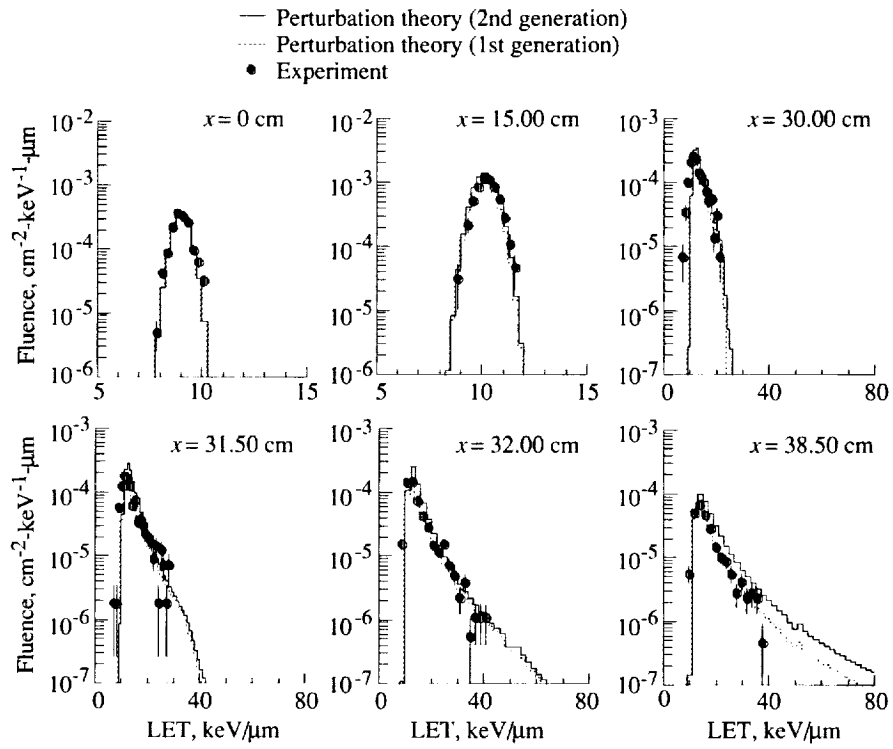


Figure 2. Differential fluence for carbon nuclei produced by neon nuclei incident on various thicknesses of water. (From ref. 6.)

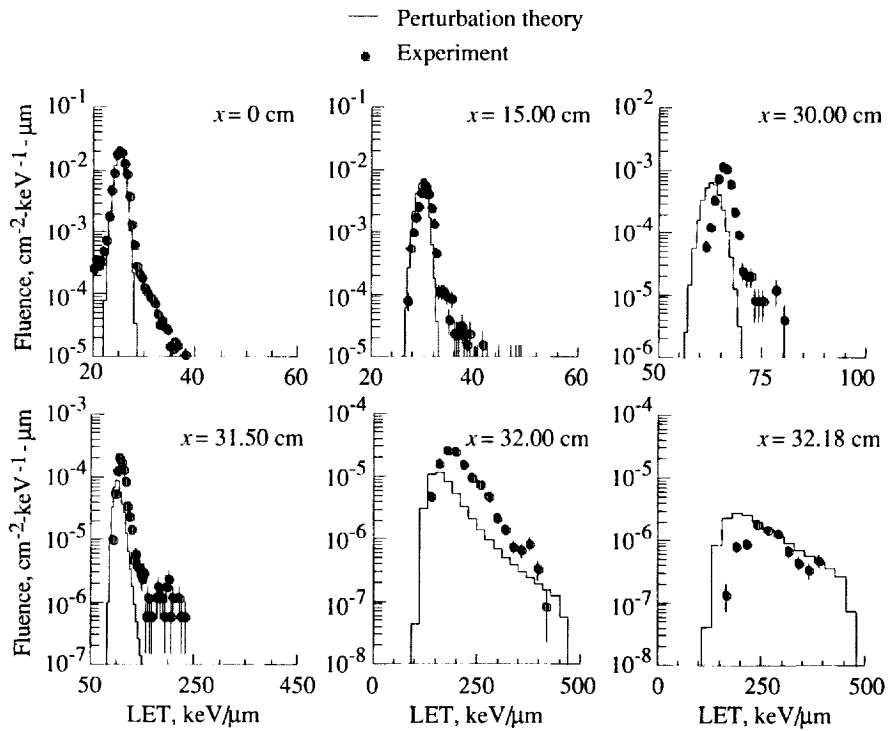
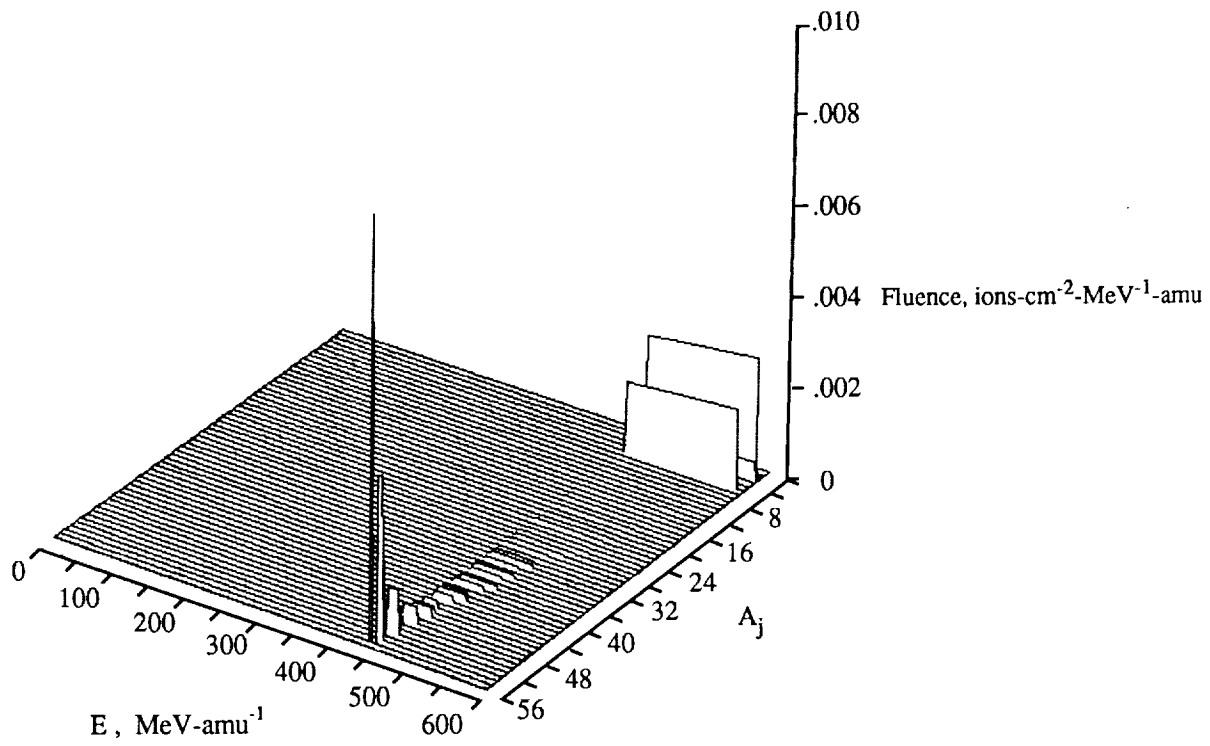
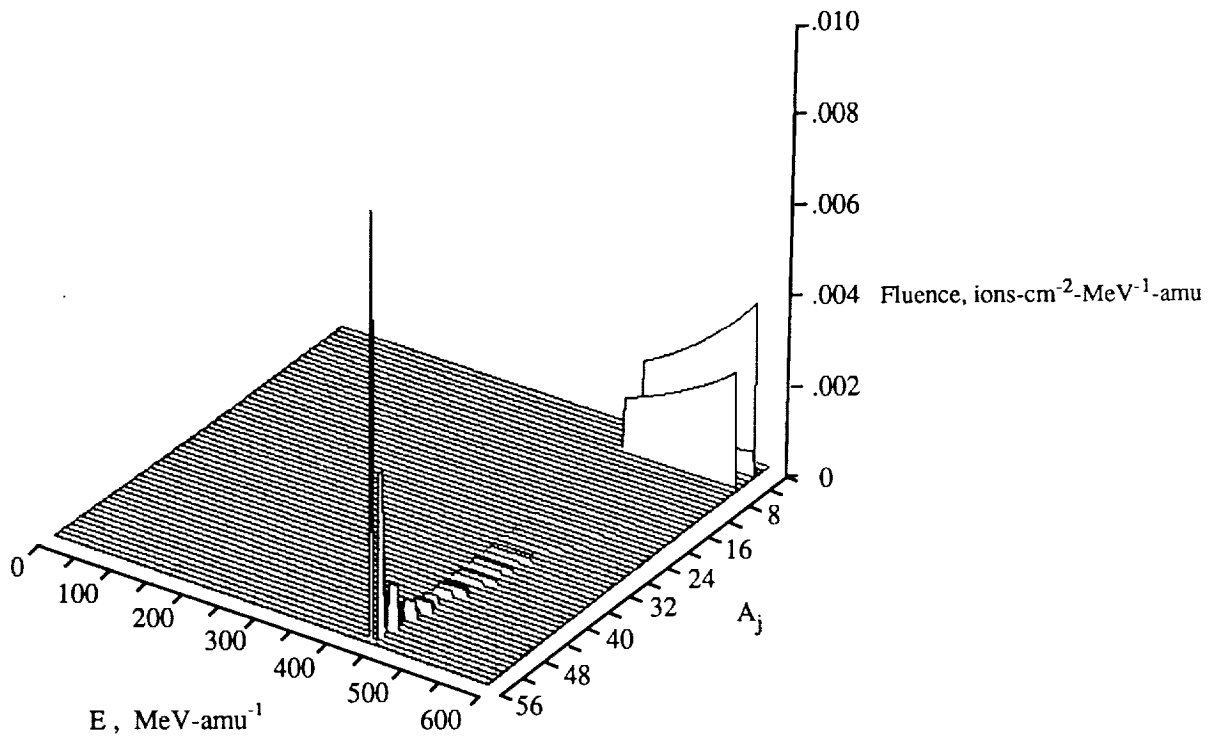


Figure 3. Differential fluence for neon nuclei incident on various thicknesses of water. (From ref. 6.)

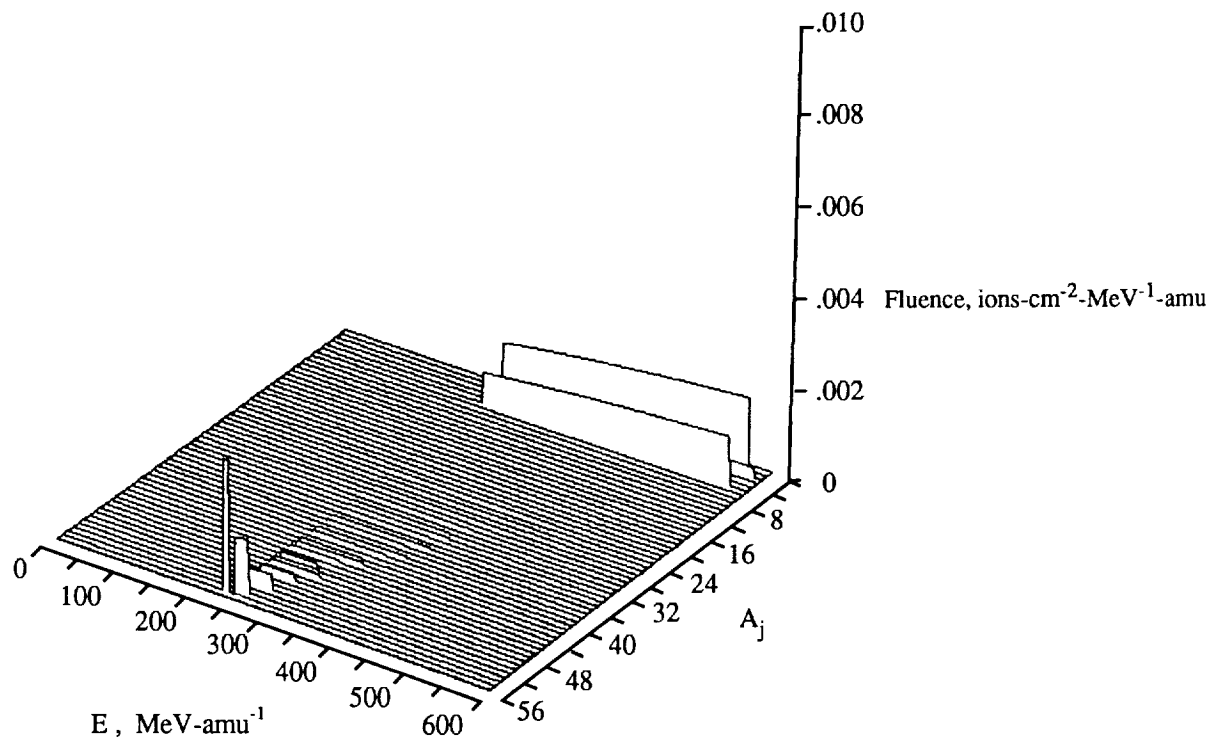


(a) Nonperturbation theory; water depth, 5 cm.

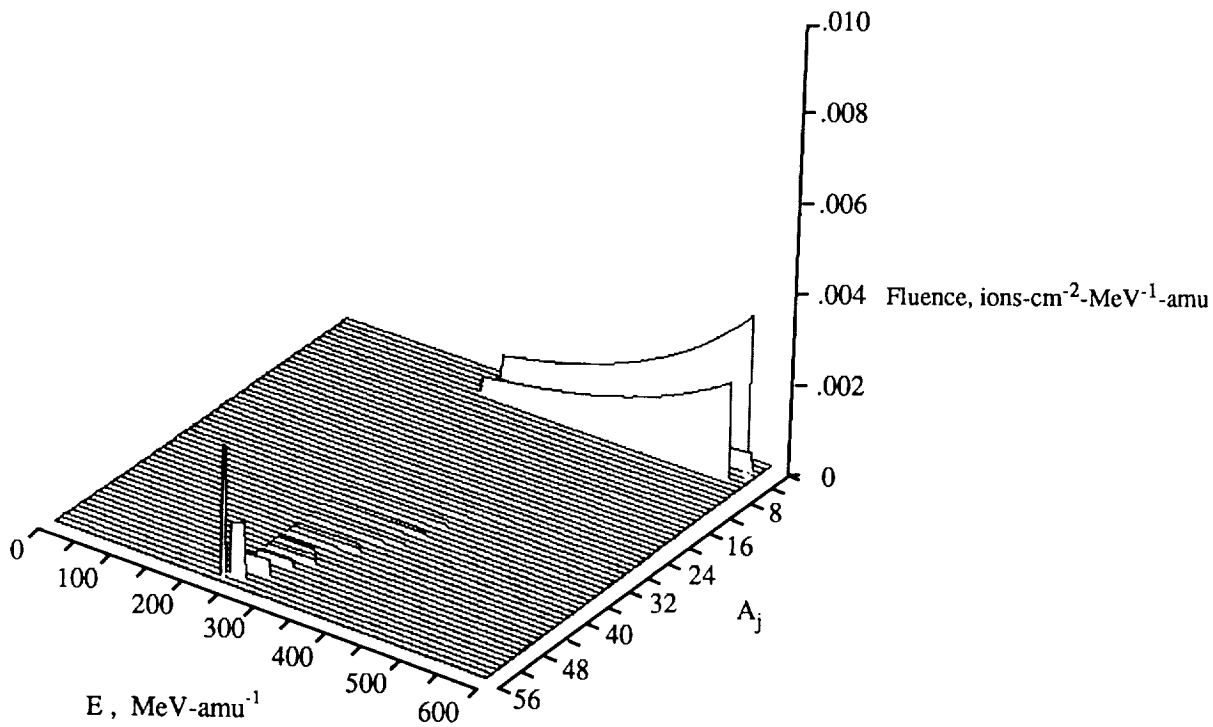


(b) Perturbation theory; water depth, 5 cm.

Figure 4. Differential fluence (first collision) for 600 MeV/amu ⁵⁶Fe beam incident on water slab from nonperturbation and perturbation theories.

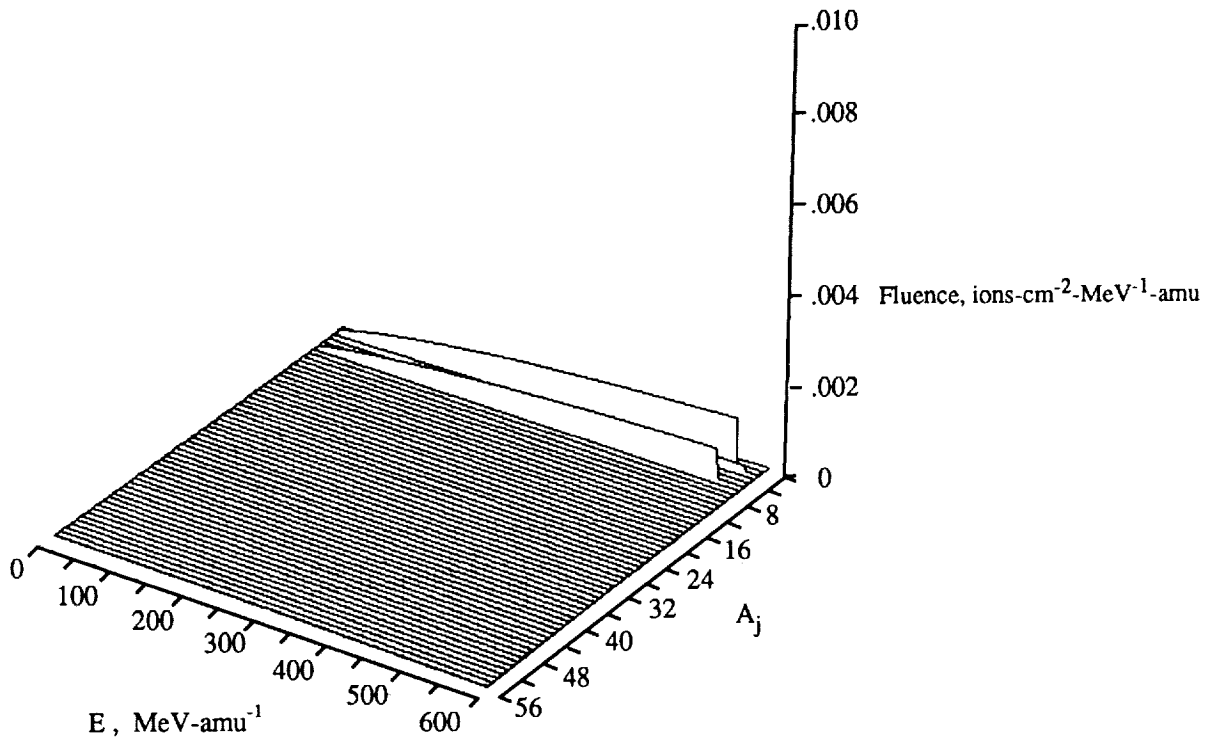


(c) Nonperturbation theory; water depth, 10 cm.

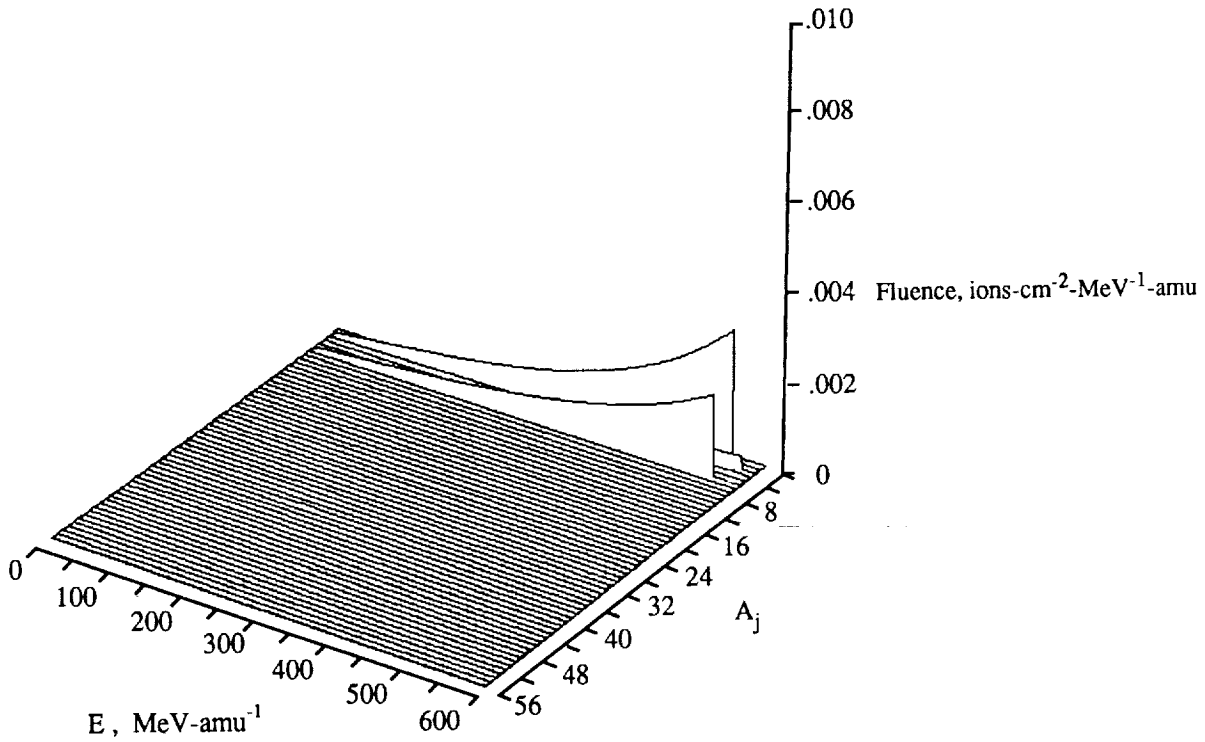


(d) Perturbation theory; water depth, 10 cm.

Figure 4. Continued.

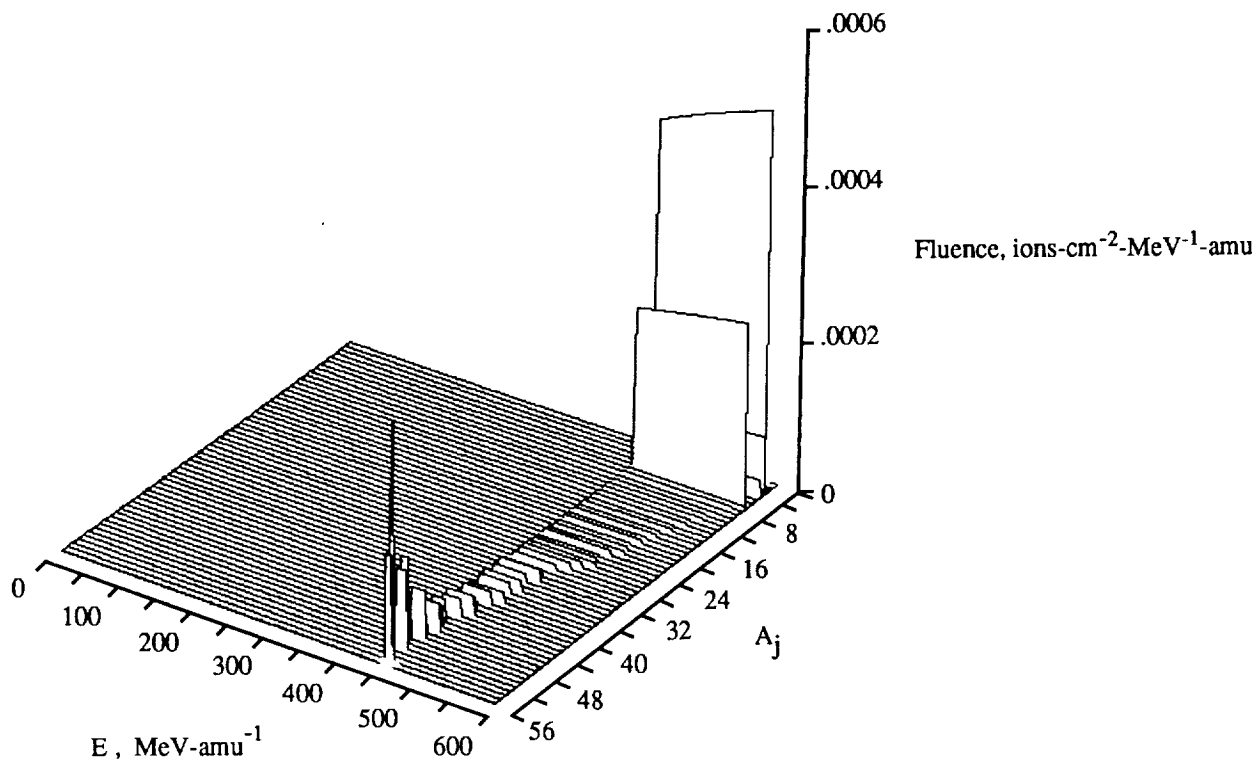


(e) Nonperturbation theory; water depth, 15 cm.

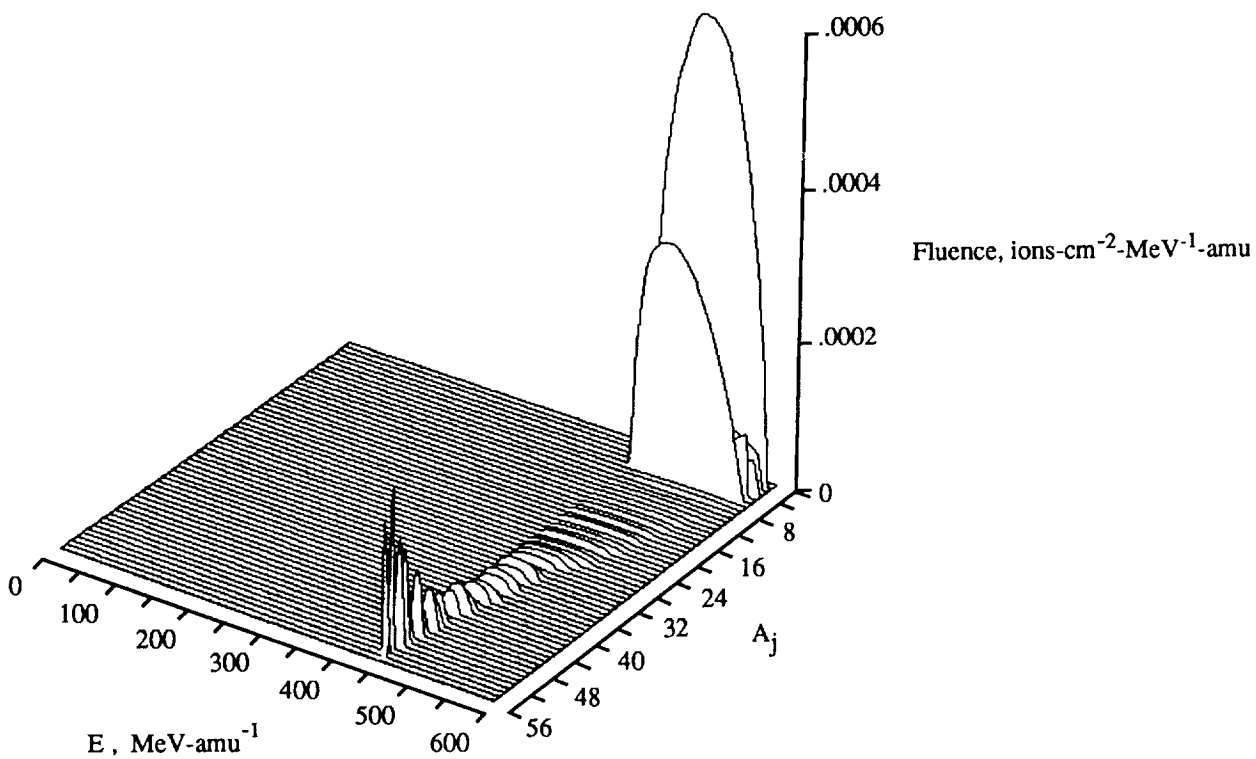


(f) Perturbation theory; water depth, 15 cm.

Figure 4. Concluded.

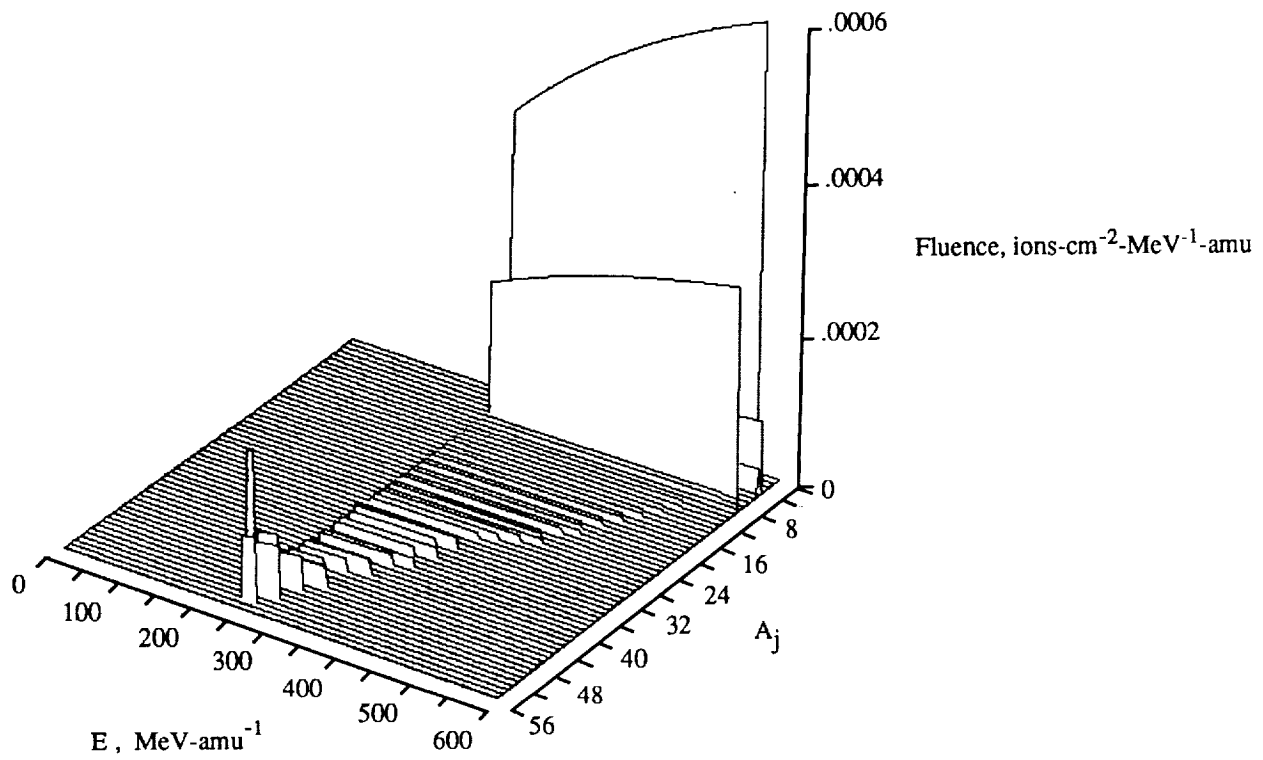


(a) Nonperturbation theory; water depth, 5 cm.

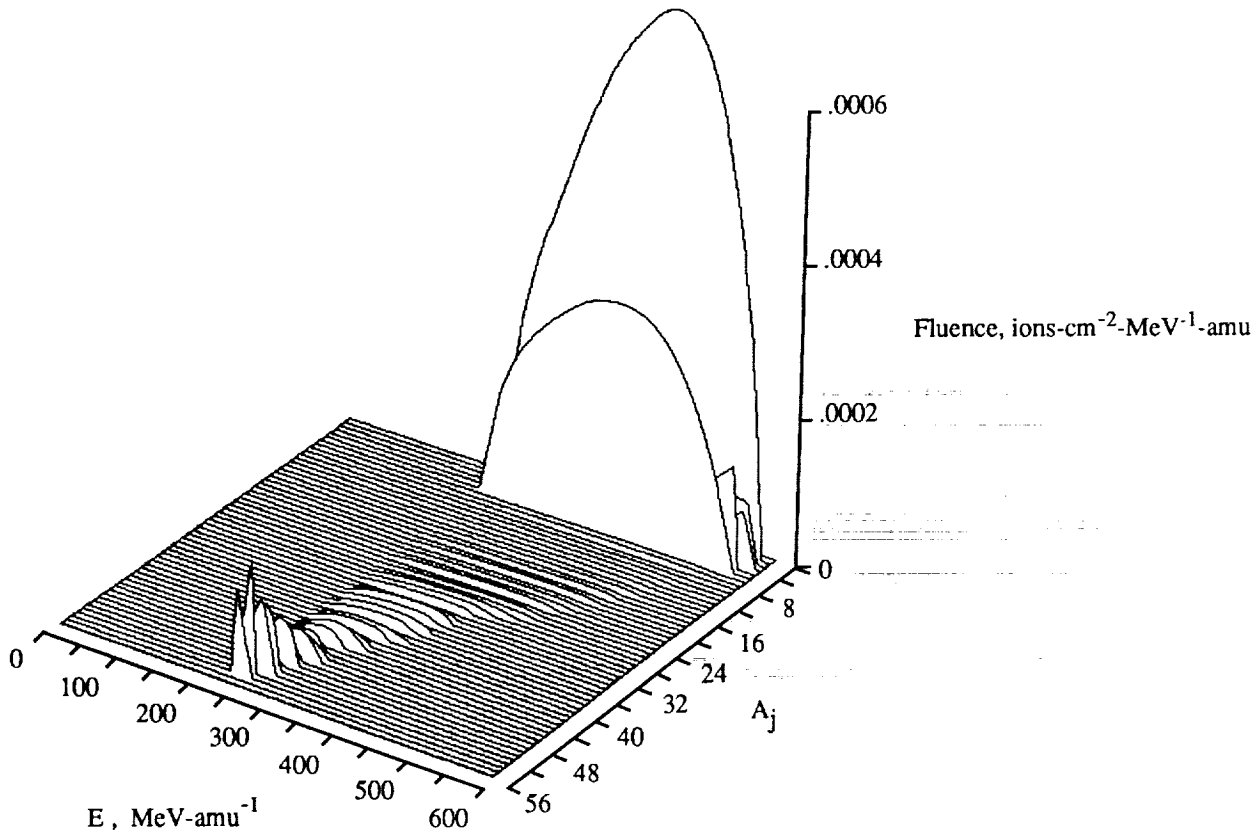


(b) Perturbation theory; water depth, 5 cm.

Figure 5. Differential fluence (second collision) for 600 MeV/amu ^{56}Fe beam incident on water slab from nonperturbation and perturbation theories.

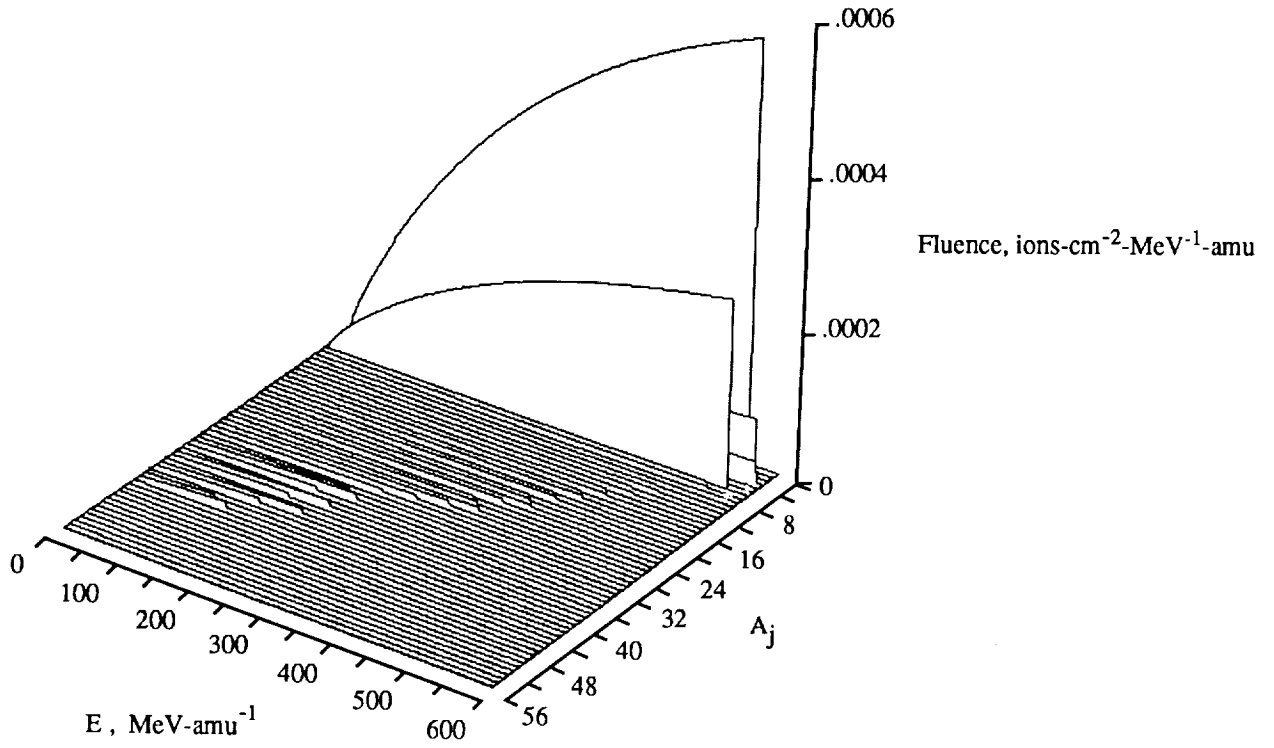


(c) Nonperturbation theory; water depth, 10 cm.

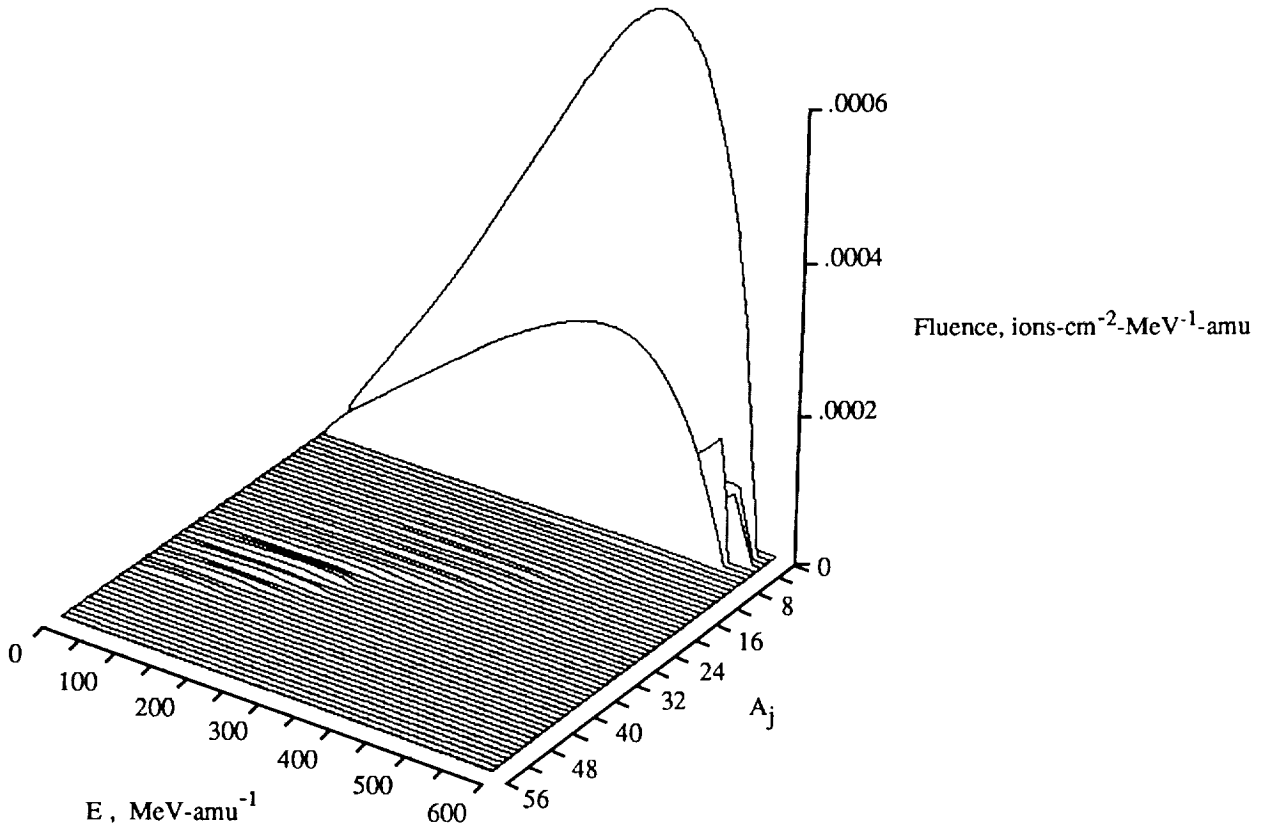


(d) Perturbation theory; water depth, 10 cm.

Figure 5. Continued.

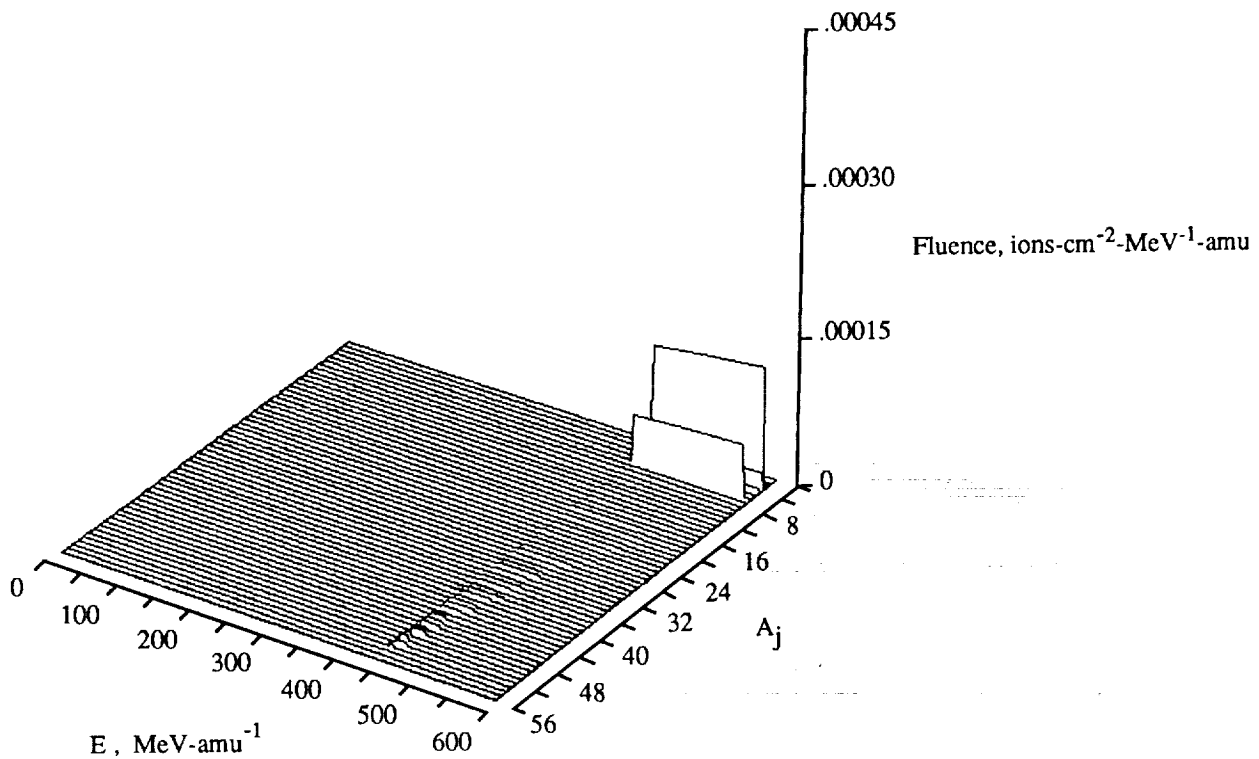


(e) Nonperturbation theory; water depth, 15 cm.

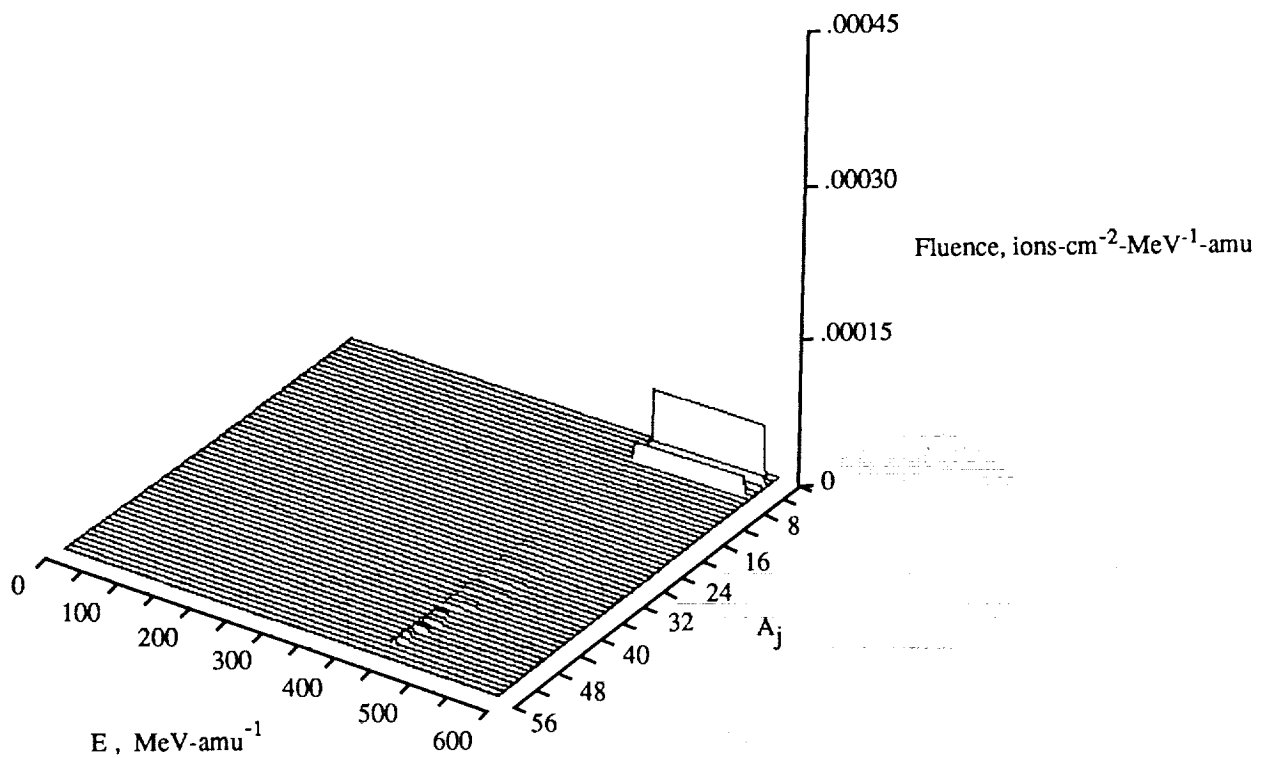


(f) Perturbation theory; water depth, 15 cm.

Figure 5. Concluded.

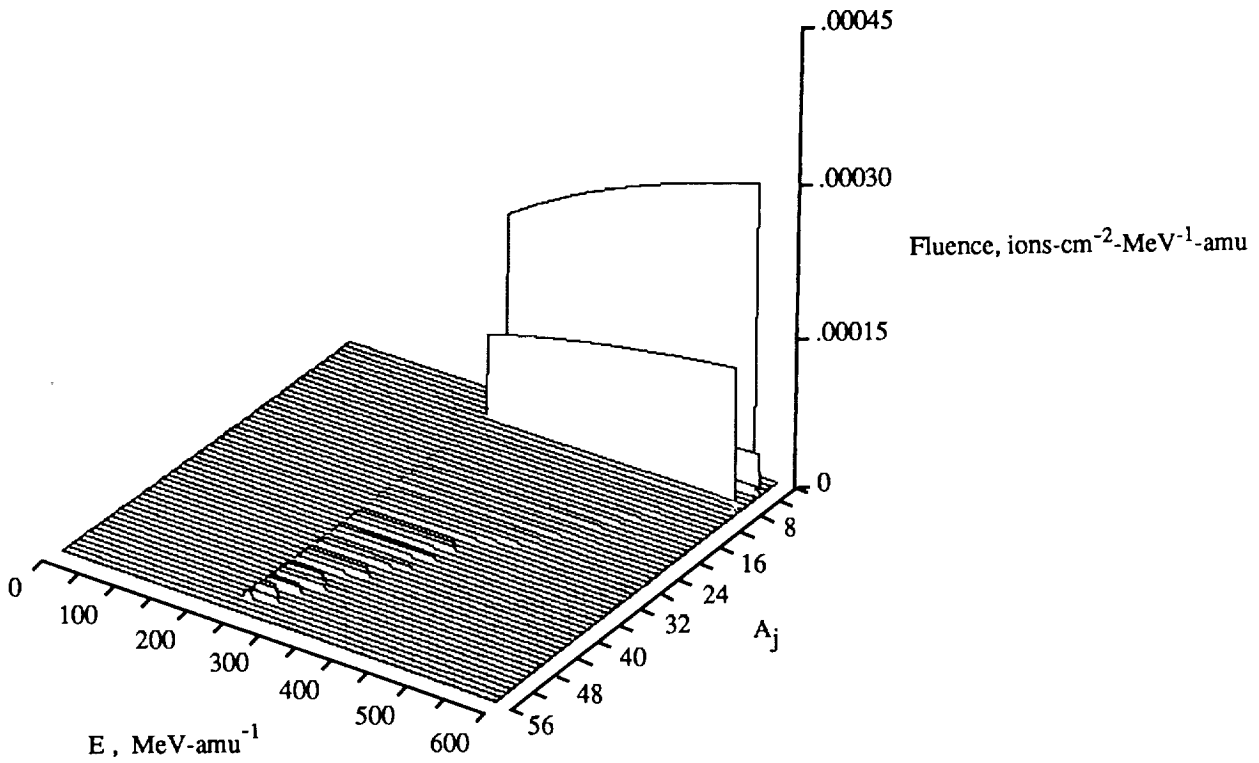


(a) Nonperturbation theory; water depth, 5 cm.

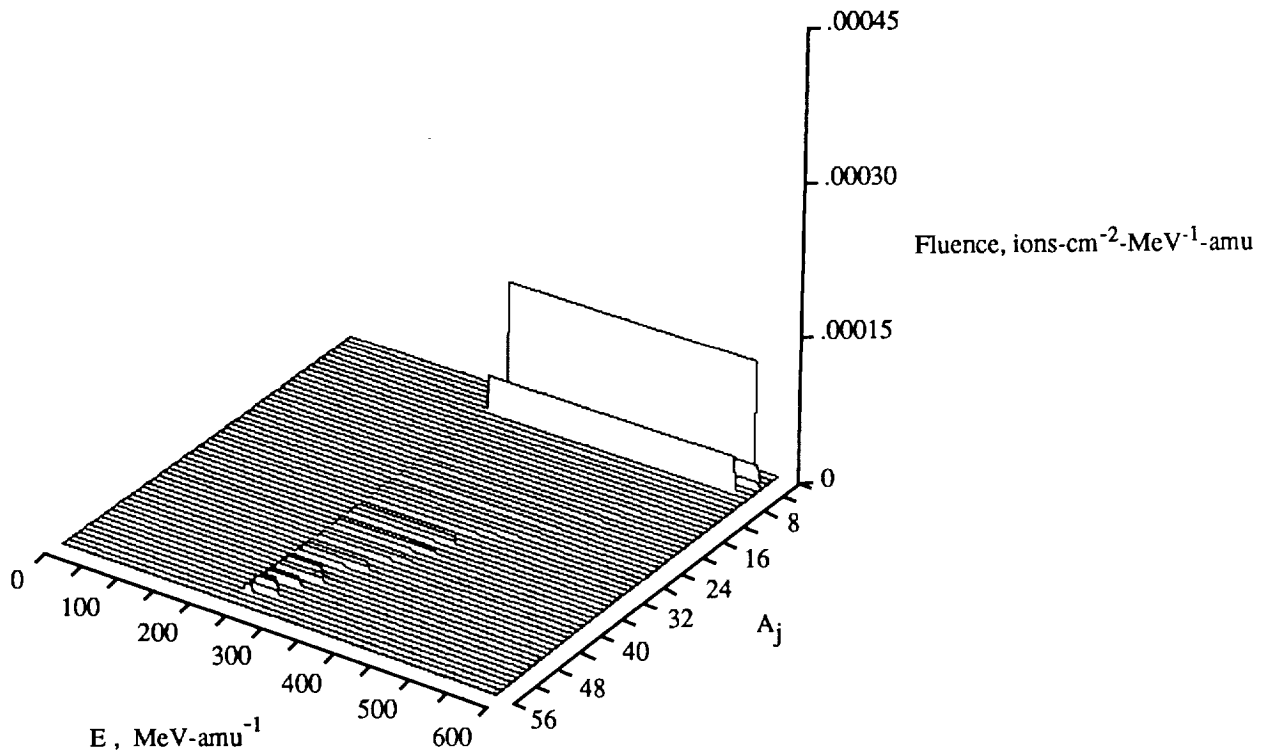


(b) Perturbation theory; water depth, 5 cm.

Figure 6. Differential fluence (higher order collision) for 600 MeV/amu ⁵⁶Fe beam incident on water slab from nonperturbation (all terms) and perturbation (third term only) theories.

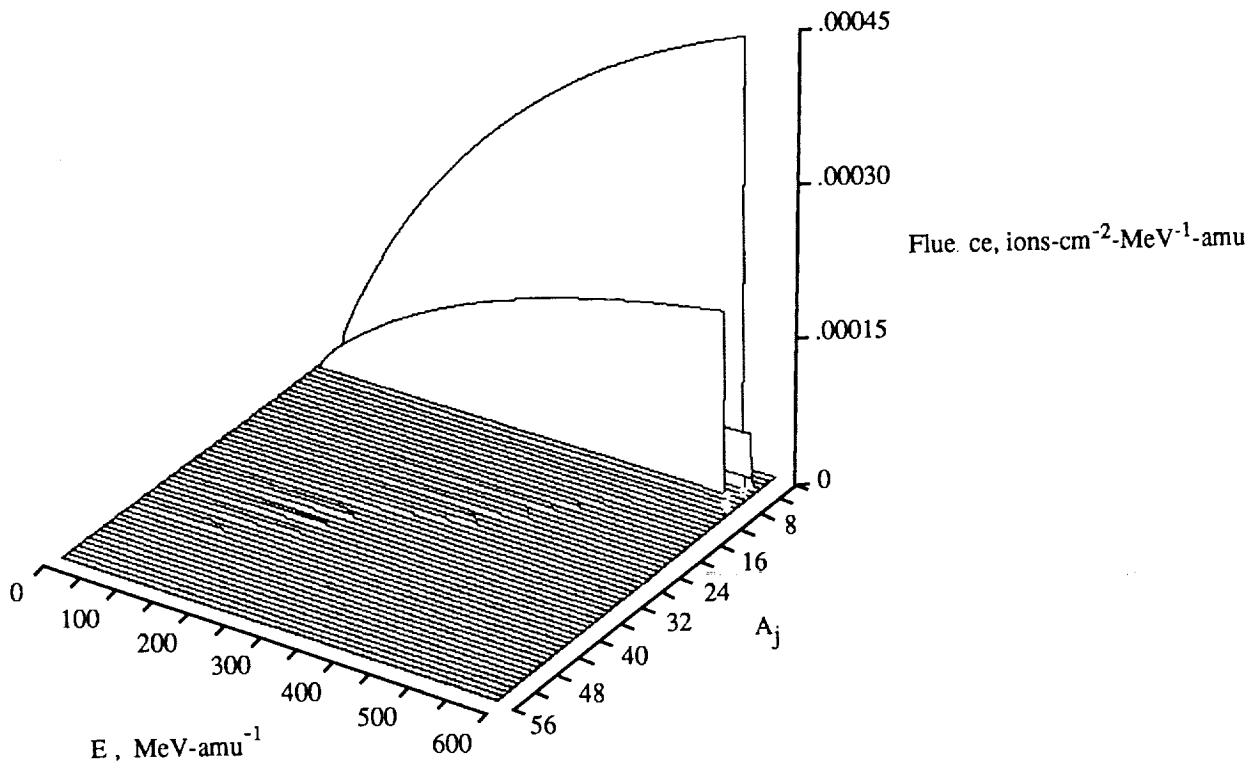


(c) Nonperturbation theory; water depth, 10 cm.

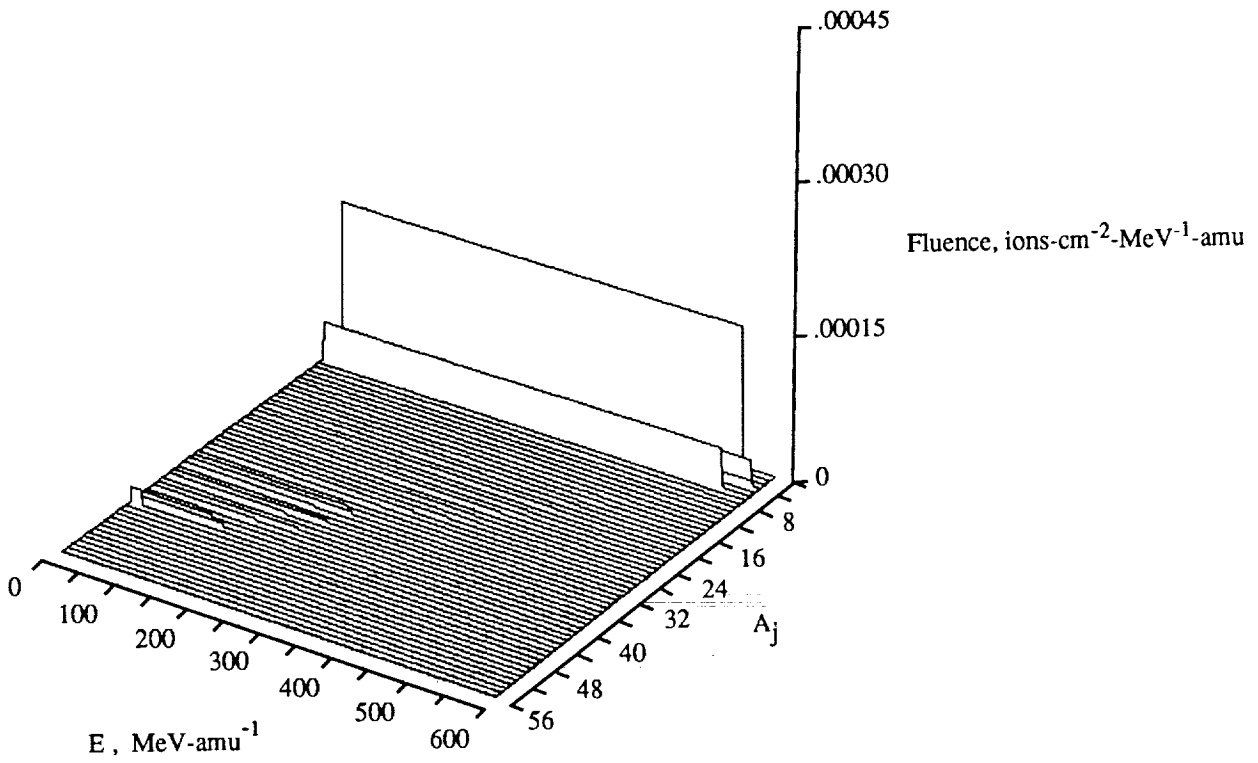


(d) Perturbation theory; water depth, 10 cm.

Figure 6. Continued.

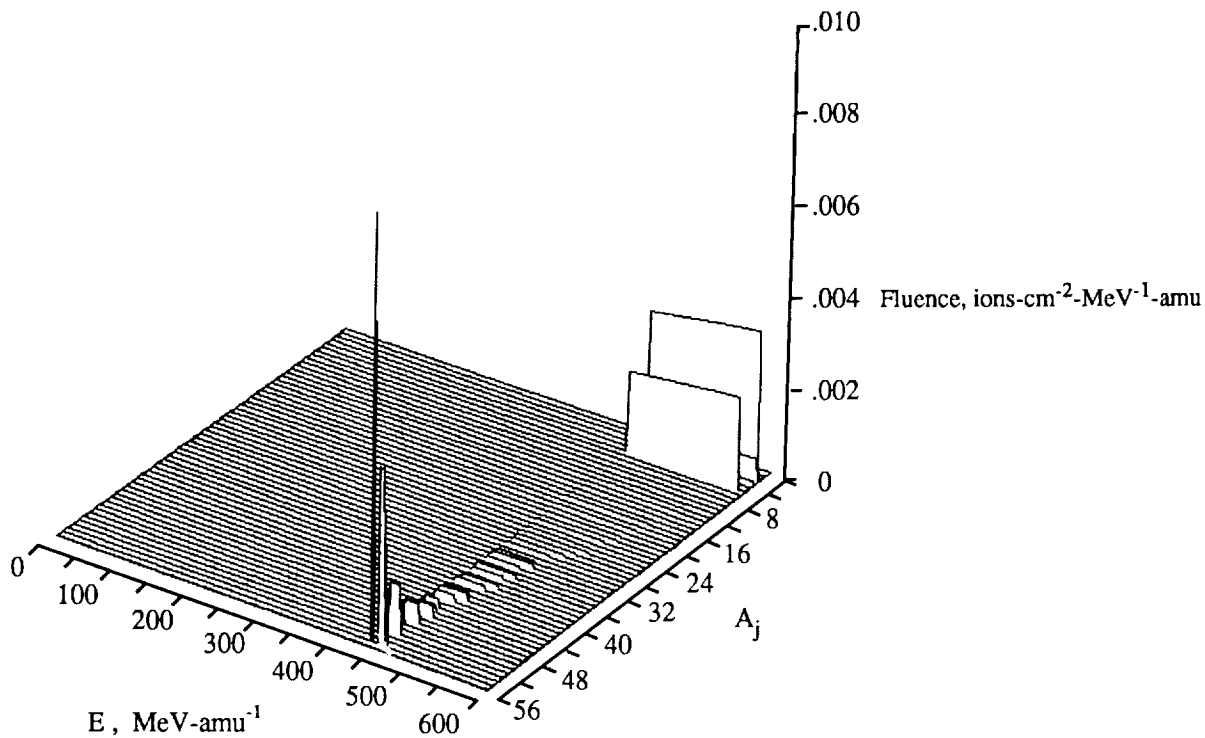


(e) Nonperturbation theory; water depth, 15 cm.

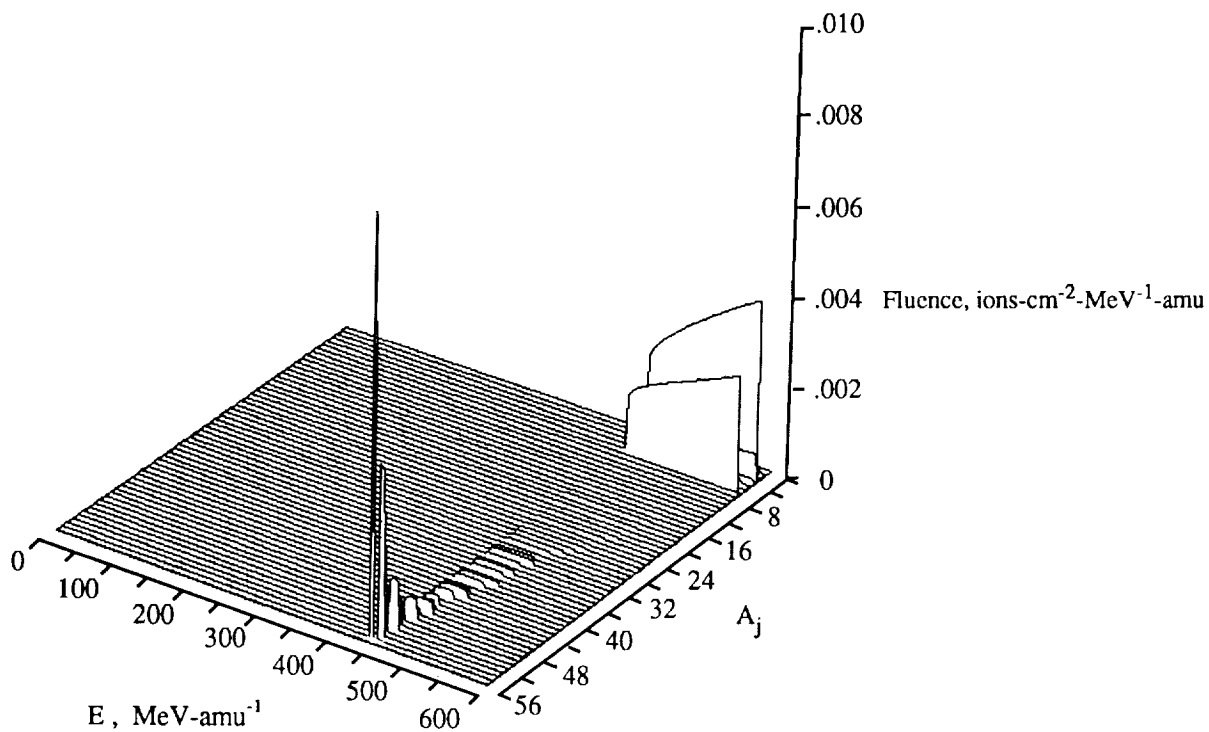


(f) Perturbation theory; water depth, 15 cm.

Figure 6. Concluded.

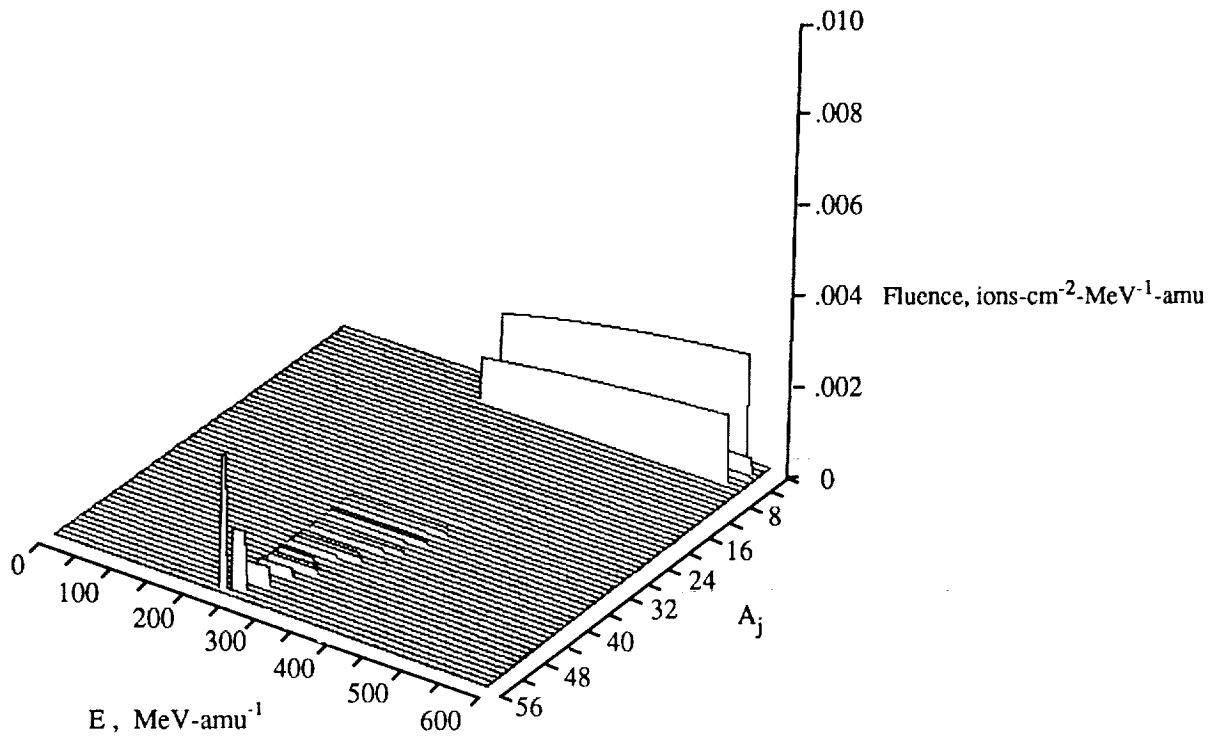


(a) Nonperturbation theory; water depth, 5 cm.

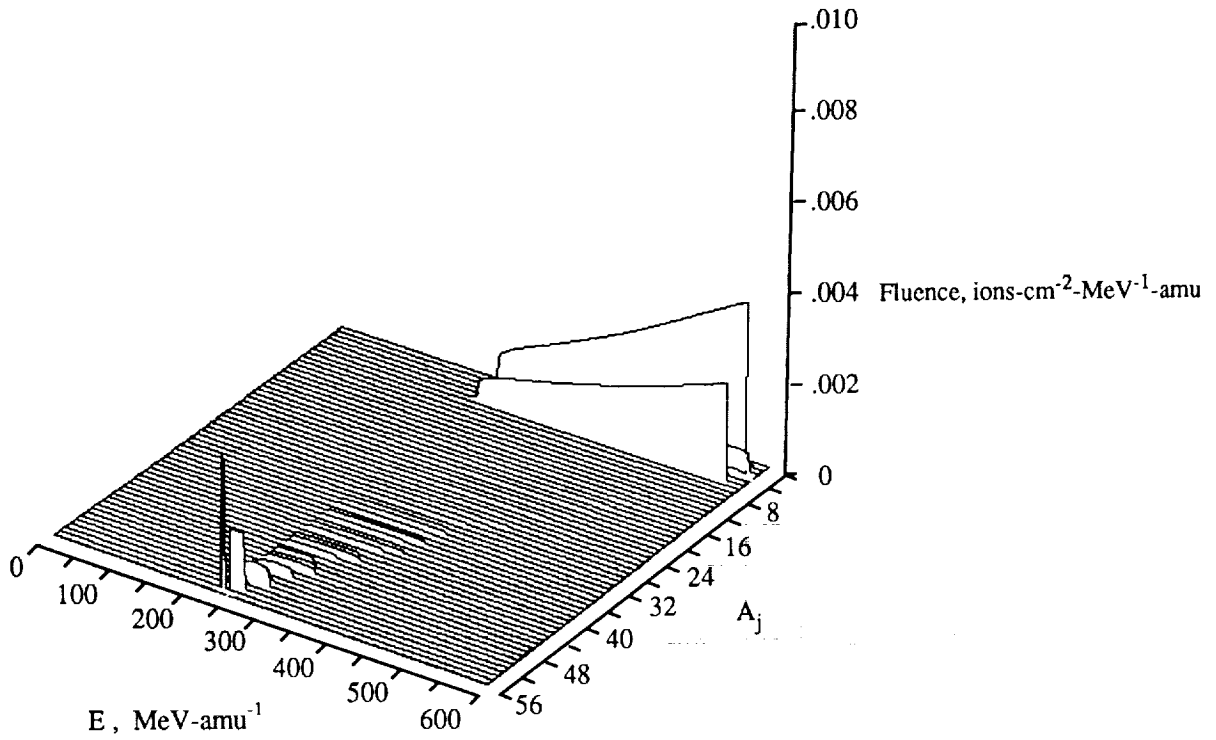


(b) Perturbation theory; water depth, 5 cm.

Figure 7. Differential fluence for 600 MeV/amu ^{56}Fe beam incident on water slab from nonperturbation (all terms) and perturbation (first three terms) theories.

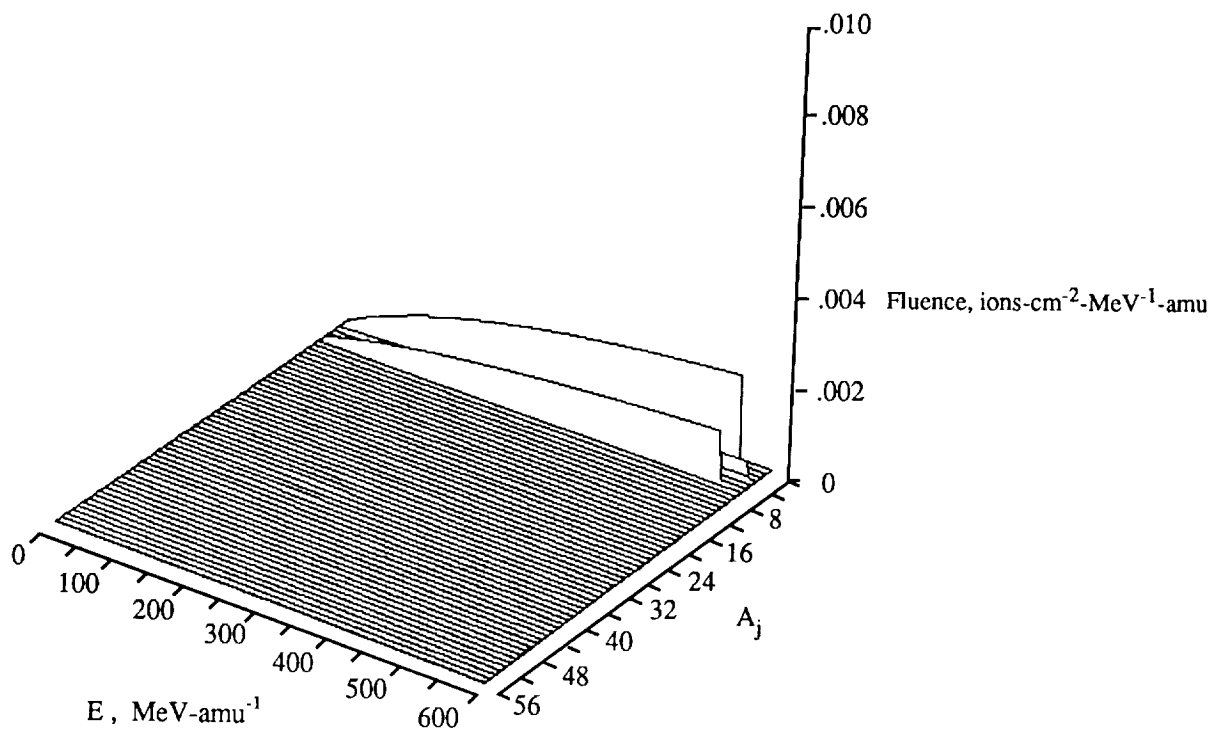


(c) Nonperturbation theory; water depth, 10 cm.

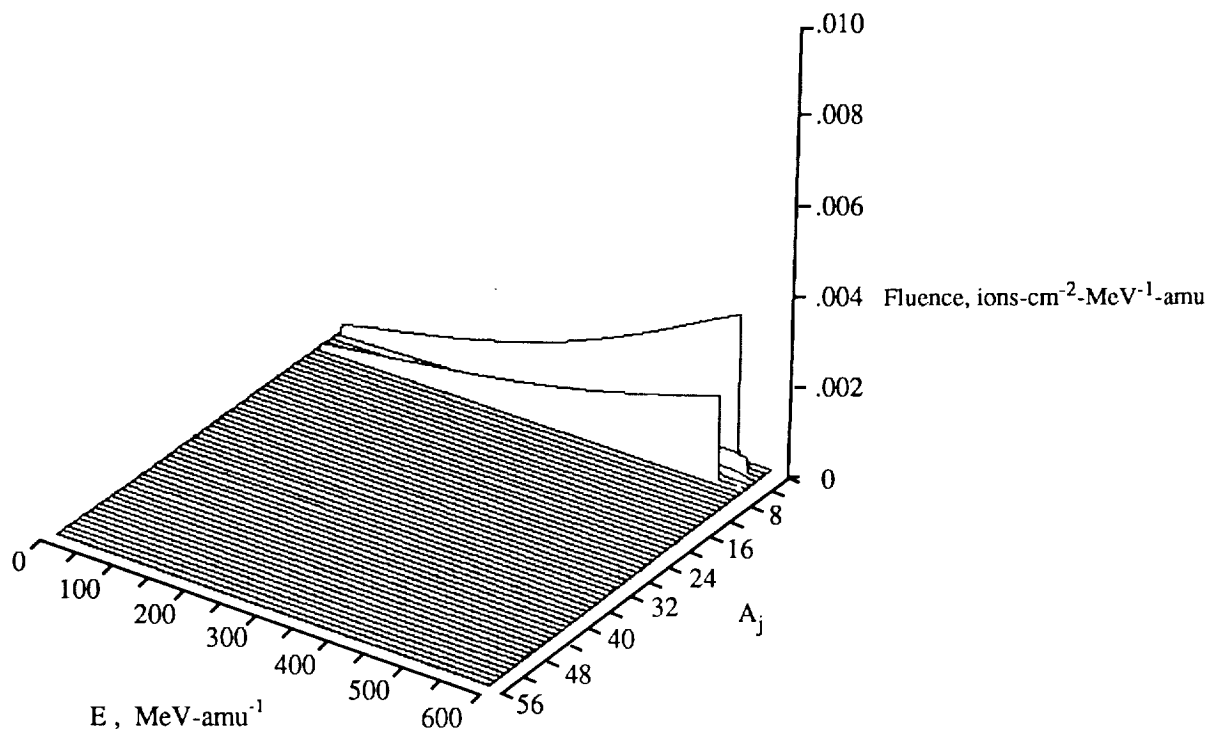


(d) Perturbation theory; water depth, 10 cm.

Figure 7. Continued.

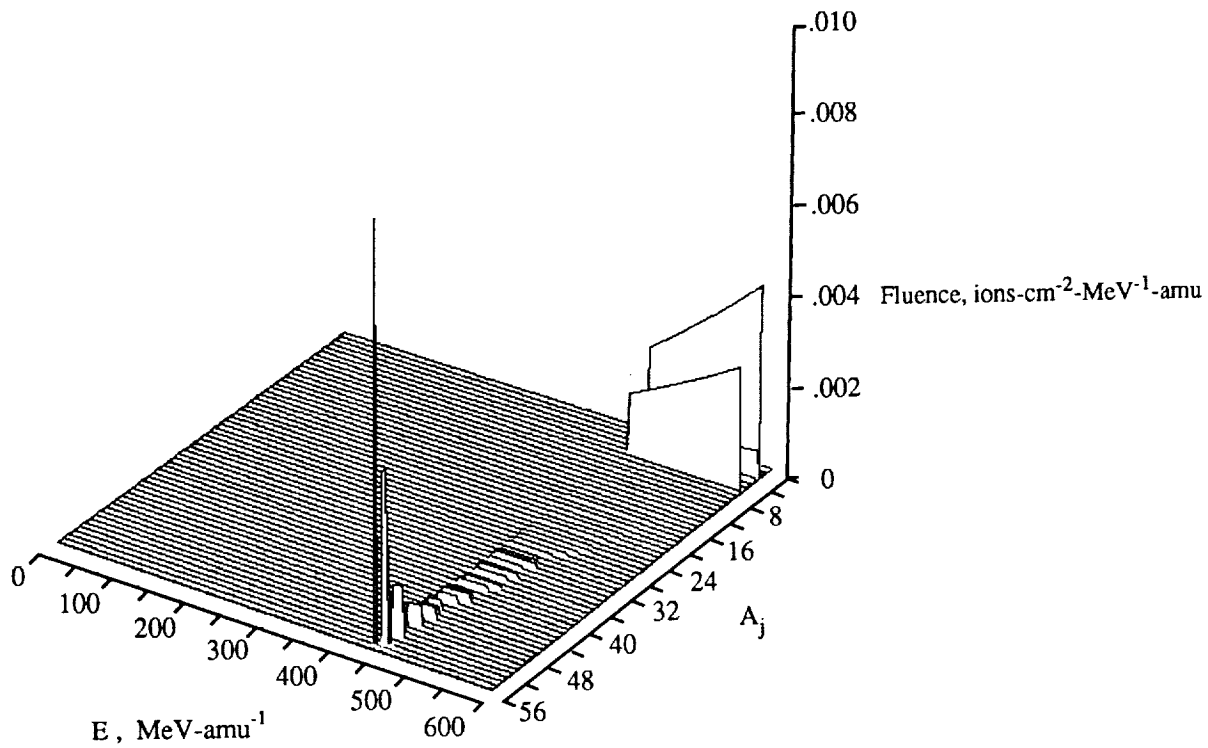


(c) Nonperturbation theory; water depth, 15 cm.

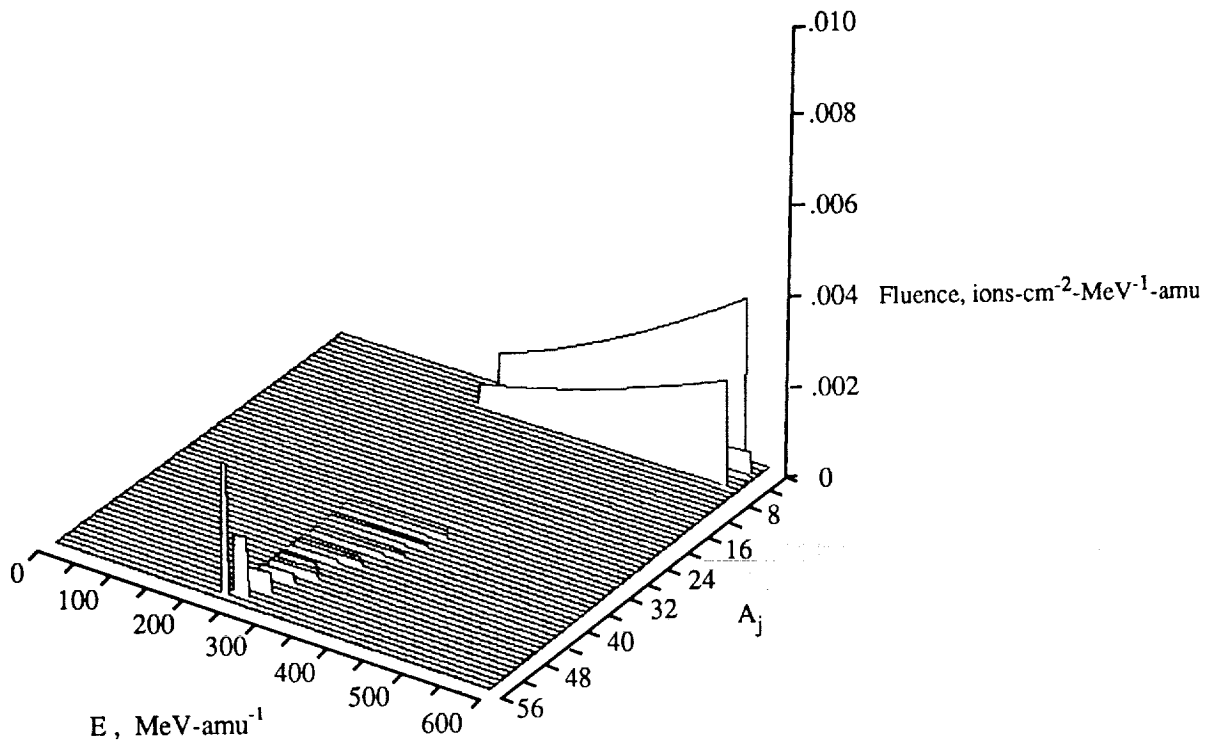


(f) Perturbation theory; water depth, 15 cm.

Figure 7. Concluded.

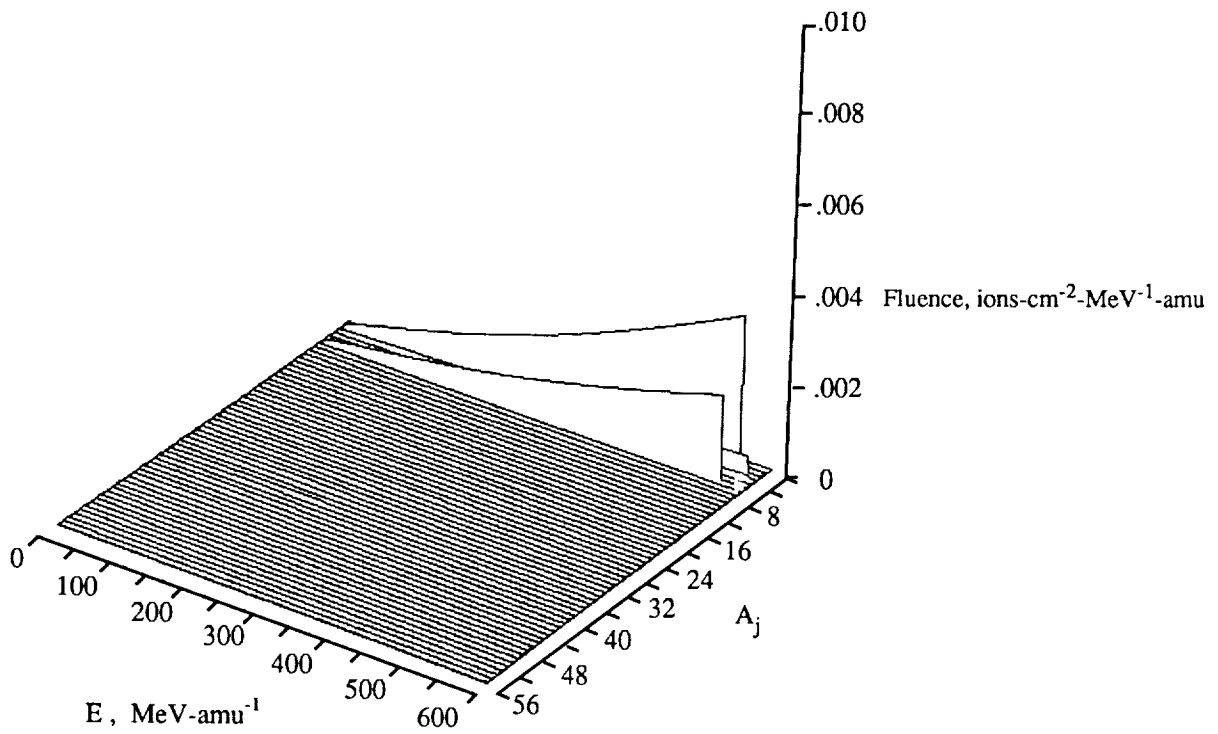


(a) Water depth, 5 cm.

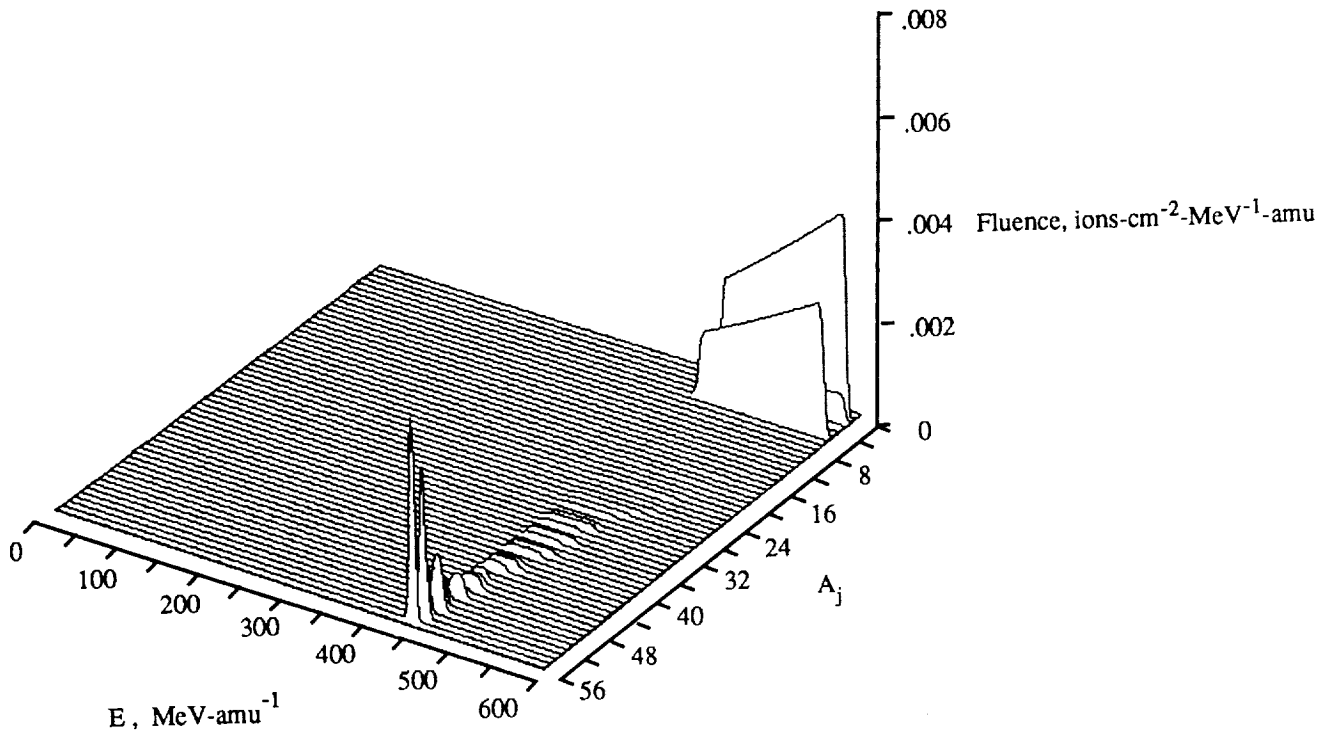


(b) Water depth, 10 cm.

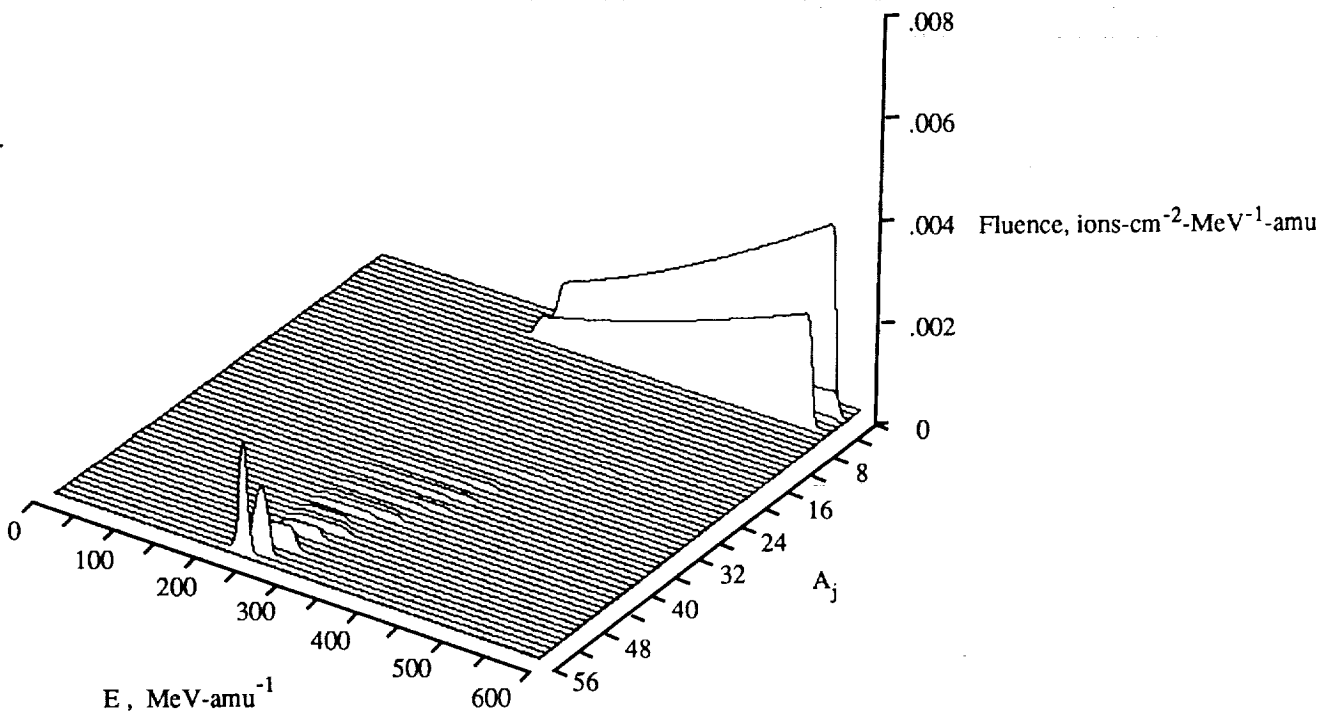
Figure 8. Differential fluence for 600 MeV/amu ⁵⁶Fe beam incident on water slab from spectral corrected nonperturbation theory.



(c) Water depth, 15 cm.
Figure 8. Concluded.

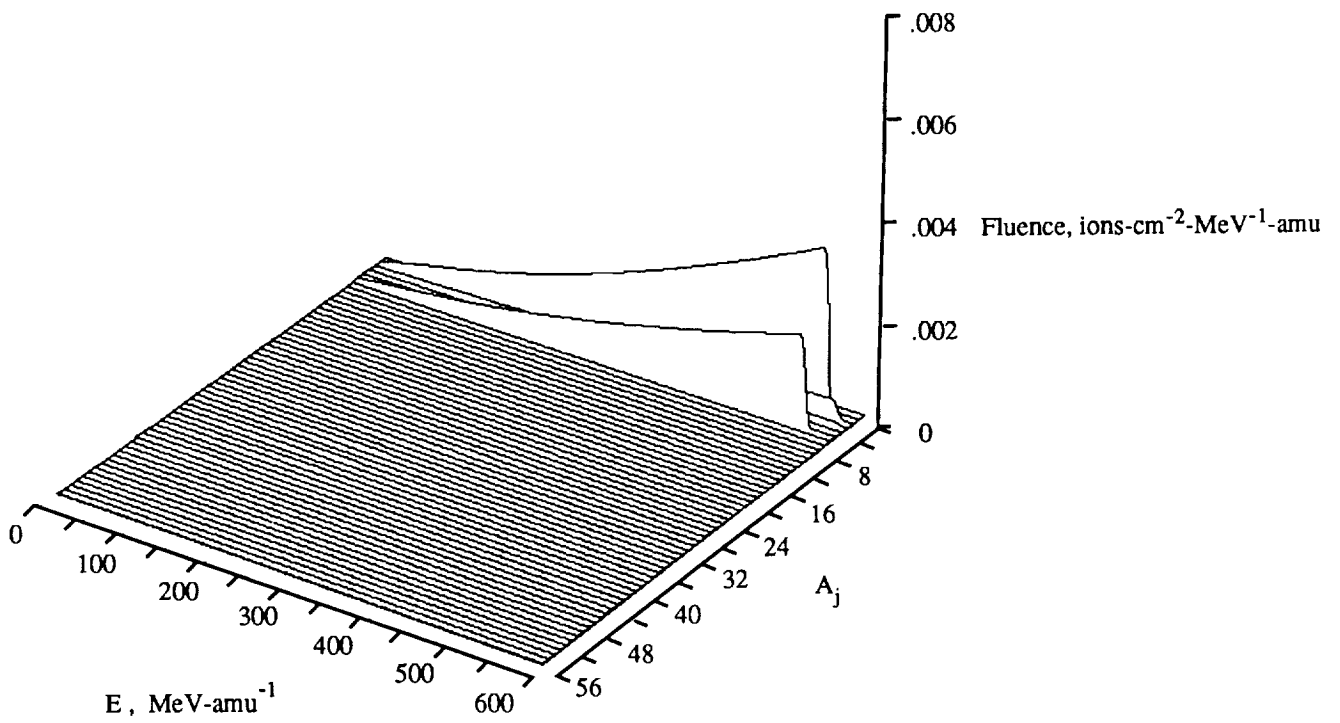


(a) Water depth, 5 cm.



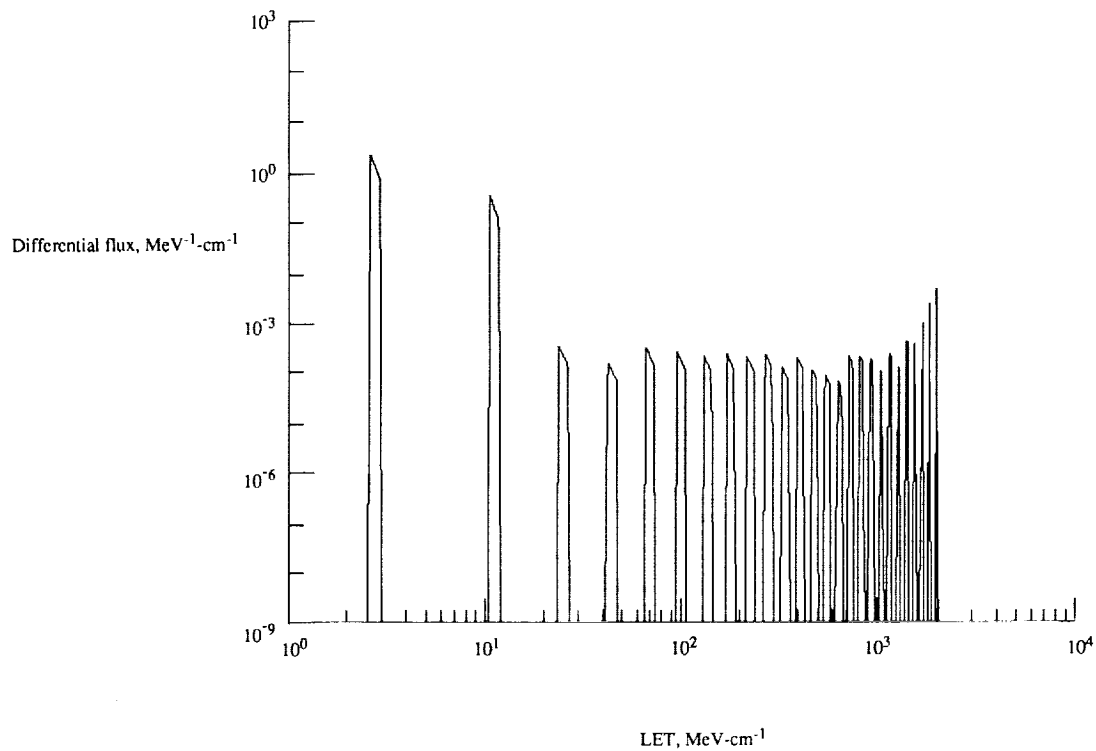
(b) Water depth, 10 cm.

Figure 9. Differential fluence for 600 MeV/amu ^{56}Fe beam with 2.5 MeV/amu standard deviation incident on water slab from perturbation theory. Primary beam not shown.

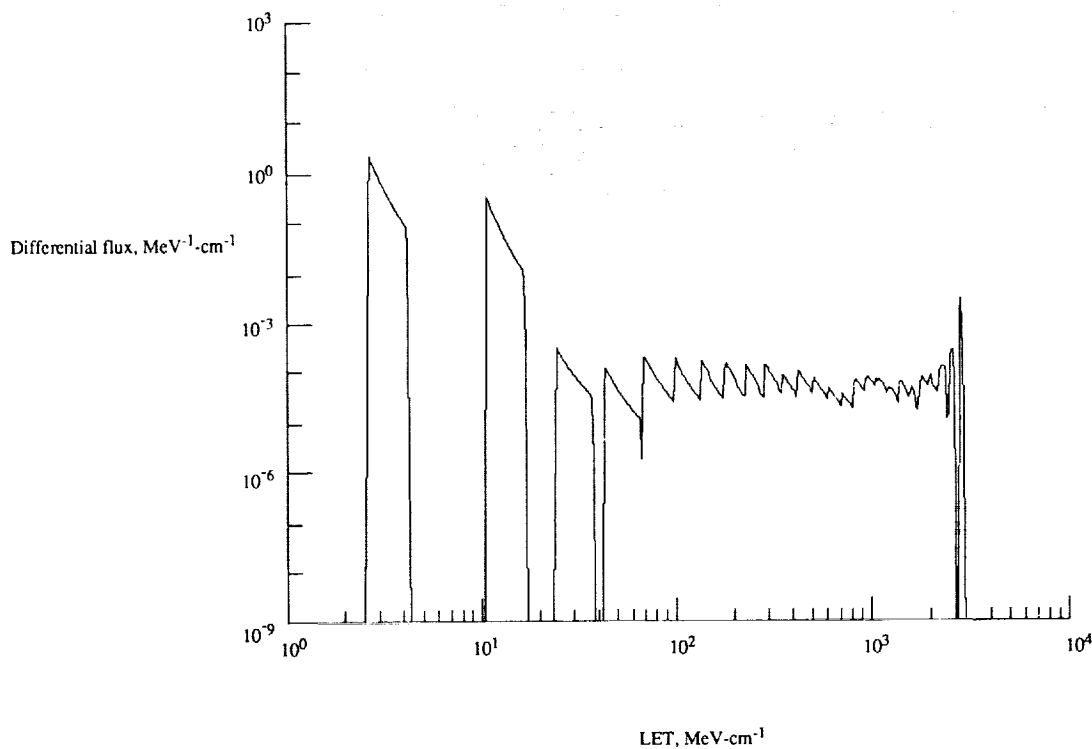


(c) Water depth, 15 cm.

Figure 9. Concluded.

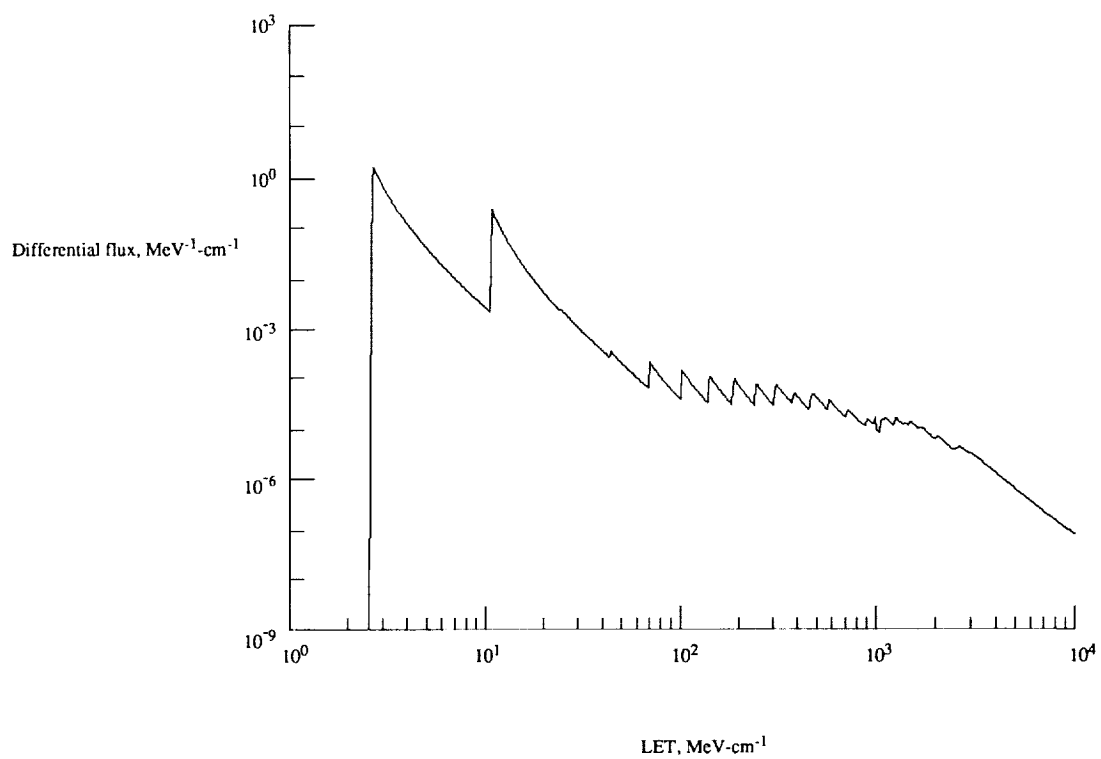


(a) Water depth, 5 cm.



(b) Water depth, 10 cm.

Figure 10. LET distribution for differential fluence for 600 MeV/amu ^{56}Fe beam with 2.5 MeV/amu standard deviation incident on water slab.



(c) Water depth, 15 cm.

Figure 10. Concluded.

REPORT DOCUMENTATION PAGE			Form Approved OMB No. 0704-0188	
Public reporting burden for this collection of information is estimated to average 1 hour per response, including the time for reviewing instructions, searching existing data sources, gathering and maintaining the data needed, and completing and reviewing the collection of information. Send comments regarding this burden estimate or any other aspect of this collection of information, including suggestions for reducing this burden, to Washington Headquarters Services, Directorate for Information Operations and Reports, 1215 Jefferson Davis Highway, Suite 1204, Arlington, VA 22202-4302, and to the Office of Management and Budget, Paperwork Reduction Project (0704-0188), Washington, DC 20503.				
1. AGENCY USE ONLY (Leave blank)	2. REPORT DATE August 1993	3. REPORT TYPE AND DATES COVERED Technical Paper		
4. TITLE AND SUBTITLE Nonperturbative Methods in HZE Ion Transport			5. FUNDING NUMBERS WU 199-45-16-11	
6. AUTHOR(S) John W. Wilson, Francis F. Badavi, Robert C. Costen, and Judy L. Shinn				
7. PERFORMING ORGANIZATION NAME(S) AND ADDRESS(ES) NASA Langley Research Center Hampton, VA 23681-0001			8. PERFORMING ORGANIZATION REPORT NUMBER L-17241	
9. SPONSORING/MONITORING AGENCY NAME(S) AND ADDRESS(ES) National Aeronautics and Space Administration Washington, DC 20546-0001			10. SPONSORING/MONITORING AGENCY REPORT NUMBER NASA TP-3363	
11. SUPPLEMENTARY NOTES Wilson, Costen, and Shinn: Langley Research Center, Hampton, VA; Badavi: Christopher Newport University, Newport News, VA.				
12a. DISTRIBUTION/AVAILABILITY STATEMENT Unclassified-Unlimited Subject Category 93			12b. DISTRIBUTION CODE	
13. ABSTRACT (Maximum 200 words) A nonperturbative analytic solution of the high charge and energy (HZE) Green's function is used to implement a computer code for laboratory ion beam transport. The code is established to operate on the Langley Research Center nuclear fragmentation model used in engineering applications. Computational procedures are established to generate linear energy transfer (LET) distributions for a specified ion beam and target for comparison with experimental measurements. The code is highly efficient and compares well with the perturbation approximations.				
14. SUBJECT TERMS Heavy ions; Transport shielding			15. NUMBER OF PAGES 26	
			16. PRICE CODE A03	
17. SECURITY CLASSIFICATION OF REPORT Unclassified	18. SECURITY CLASSIFICATION OF THIS PAGE Unclassified	19. SECURITY CLASSIFICATION OF ABSTRACT	20. LIMITATION OF ABSTRACT	